IEEE Access
Multidisciplinary | Rapid Review | Open Access Journal

Received July 18, 2017, accepted August 3, 2017, date of publication August 24, 2017, date of current version March 28, 2018.

Digital Object Identifier 10.1109/ACCESS.2017.2741578

Energy Management and Optimization Methods for Grid Energy Storage Systems

RAYMOND H. BYRNE[1], (Fellow, IEEE), TU A. NGUYEN[1], (Member, IEEE), DAVID A. COPP[1], (Member, IEEE), BABU R. CHALAMALA[1], (Fellow, IEEE), AND IMRE GYUK[2]

[1]Sandia National Laboratories, Albuquerque, NM 87185, USA
[2]U.S. Department of Energy, Washington, DC 20585, USA

Corresponding author: Raymond H. Byrne (rhbyrne@sandia.gov)

This work was supported by the Energy Storage Program at the U.S. Department of Energy Office of Electricity Delivery and Energy Reliability.

ABSTRACT Today, the stability of the electric power grid is maintained through real time balancing of generation and demand. Grid scale energy storage systems are increasingly being deployed to provide grid operators the flexibility needed to maintain this balance. Energy storage also imparts resiliency and robustness to the grid infrastructure. Over the last few years, there has been a significant increase in the deployment of large scale energy storage systems. This growth has been driven by improvements in the cost and performance of energy storage technologies and the need to accommodate distributed generation, as well as incentives and government mandates. Energy management systems (EMSs) and optimization methods are required to effectively and safely utilize energy storage as a flexible grid asset that can provide multiple grid services. The EMS needs to be able to accommodate a variety of use cases and regulatory environments. In this paper, we provide a brief history of grid-scale energy storage, an overview of EMS architectures, and a summary of the leading applications for storage. These serve as a foundation for a discussion of EMS optimization methods and design.

INDEX TERMS Energy storage system (ESS), energy management system (EMS), battery energy storage system (BESS), optimization methods, optimal control, linear programming (LP), mixed integer linear programming (MILP), battery management system (BMS).

I. INTRODUCTION

Energy storage has the potential to significantly increase the efficiency, stability, and resiliency of the electric power grid. Today, electricity generation must always be in dynamic balance with load. With the increasing role of variable generation and changing demand profiles, grid operators have limited resources to maintain this dynamic balance. Energy storage, if suitably deployed, gives the grid operators a flexible and fast responding resource to effectively manage variability in generation and demand.

For 2017, the North American Electric Reliability Corporation (NERC) projected peak demand is 839 GW for the three major interconnections in the United States [1]. However, the amount of installed energy storage capacity, including large pumped hydro plants, is small relative to the amount of generation capacity. The U.S. electric power grid contains approximately 24 GW of energy storage with 0.6 GW from electrochemical (battery) storage, 0.8 GW from thermal storage, and the remainder from pumped hydro [2]. The amount of energy storage deployed in the United States thus represents only about 2.9% of peak demand, and a similar situation exists worldwide. According to the Global Energy Storage Database [2], approximately 96% of worldwide energy storage capacity is in pumped hydro facilities. Table 2 provides a summary of the installed energy storage capacity around the world.

Energy storage is capable of providing a number of grid benefits [3], [4], which are typically categorized based on the time scale. On a slower time scale are energy supply interactions, where large amounts of energy are supplied or pulled from the grid. These are often referred to as ''energy'' applications. Examples include renewable energy time shift and energy arbitrage in market areas. On the other hand, ''power'' applications normally transpire on a much faster time scale and are employed to support real-time control of the electric power grid. Examples include voltage support and small signal stability. A summary of grid benefits, divided into energy and power applications, is summarized in Table 3.

TABLE 1. Nomenclature.

AC	Alternating Current
ACE	Area Control Error
AGC	Automatic Generation Signal
BMS	Battery Management System
CAES	Compressed Air Energy Storage
CAISO	California Independent System Operator
DAM	Day Ahead Market
DC	Direct Current
DMS	Device Management System
DNP	Distributed Network Protocol
DR	Demand Response
DSM	Demand Side Management
EMS	Energy Management System
ERCOT	Electric Reliability Council of Texas
FERC	U.S. Federal Energy Regulatory Commission
HVAC	Heating, Ventilation, and Air Conditioning
ISO	Independent System Operator
LMP	Locational Marginal Price
LP	Linear Program
LQE	Linear Quadratic Estimator
LQR	Linear Quadratic Regulator
MILP	Mixed Integer Linear Program
MISO	Midcontinent Independent System Operator
MPC	Model Predictive Control
NERC	North American Electric Reliability Corporation
NPV	Net Present Value
O&M	Operation and Maintenance
PCS	Power Conversion System
PF	Power Factor
PI	Proportional-Integral
PJM	PJM Interconnection LLC
PV	Photovoltaic
RMS	Root Mean Square
RoCoF	Rate of Change of Frequency
RTM	Real Time Market
RTO	Regional Transmission Operator
SMES	Superconducting Magnetic Energy Storage
SOC	State of Charge
SOH	State of Health
TCP	Transmission Control Protocol
T&D	Transmission and Distribution
VRFB	Vanadium Redox Flow Battery

TABLE 2. World energy storage installed operational capacity [2].

Technology	Projects	Rated Power (MW)
Electro-chemical storage	737	1,775
Pumped hydro storage	327	169,208
Thermal storage	196	3,321
Electro-mechanical storage	50	1,568
Hydrogen storage	8	14

Since the operation of an energy storage system often involves deciding which service to provide at each time interval to maximize revenue or grid benefit, it is naturally formulated as an optimization problem.

In the literature, there have been a number of studies investigating the benefits of energy storage for generation, transmission, and distribution applications. In [5], a theoretical framework of planning and control is proposed to maximize the profit of battery energy storage systems for primary frequency control. The maximum potential revenue in different market areas from energy arbitrage and frequency regulation is investigated in [6]–[11]. This includes the formulation of the revenue maximization problem for different markets. A real-time optimal dispatch algorithm for energy storage is proposed in [12] to maximize revenue from energy arbitrage in the day-ahead electricity market and to provide transmission congestion relief. The financial benefit of battery energy storage for distribution system upgrade deferral is presented in [13]. Optimal operation of battery energy storage for mitigating photovoltaic (PV) variability and reducing transformer losses is studied in [14]. A review of energy storage benefits for grid applications is presented in [4] and [15]. There has been a significant amount of work on battery management systems (BMSs) [15]–[18], along with several reviews [19], [20].

TABLE 3. Summary of energy storage applications.

Energy Applications	Power Applications
Arbitrage	Frequency regulation
Renewable energy time shift	Voltage support
Demand charge reduction	Small signal stability
Time-of-use charge reduction	Frequency droop
T&D upgrade deferral	Synthetic inertia
Grid resiliency	Renewable capacity firming

For the efficient operation of large scale energy storage systems, there are two main engineering challenges that need to be adequately addressed:

- Optimal scheduling of grid energy storage to guarantee safe operation while delivering the maximum benefit.
- Coordination of multiple grid energy storage systems that vary in size and technology.

In order to solve these engineering challenges, sophisticated energy management systems (EMSs) are required to monitor and optimally control each energy storage system, as well as to interoperate multiple energy storage systems.

In this paper, we provide a review of energy management systems for grid energy storage. This includes an overview of EMS architectures and optimization methods to enable efficient utilization of storage systems. While this review focuses on optimal management of energy storage, closely related applications include:

- virtual power plant operation, which typically involves control of distributed generation, demand response, and energy storage to emulate the characteristics of a traditional generator [21]–[23],
- managing distributed energy resources [24], and decentralized control of distributed energy resources via microgrids [25]–[28],
- and energy management for vehicle-to-grid and grid-to-vehicle applications of plug-in electric vehicles [29], [30].

The review is organized into five topic areas. A brief history of grid-scale energy storage deployments is presented in Section II. Section III provides an overview of EMS architectures. Section IV reviews ''energy'' applications while Section V covers ''power'' applications. Section VI outlines the optimal operation of energy storage. This includes a discussion of models, optimization approaches, the optimization formulation for market areas, the optimization approach for vertically integrated utilities, and a review of behind-the-meter control algorithms. Acronyms are defined in Table 1.

II. HISTORY OF GRID ENERGY STORAGE

The first pumped hydro facilities were built in the 1890's in Switzerland and Italy to support industrial loads [31]. In the early 20^{th} century, pumped hydro storage systems were integrated into the power grid of several European countries primarily to improve the operational efficiency of thermal power plants [31]. The first large-scale energy storage project deployed in the United States was a pumped hydro facility near New Milford, Connecticut [32]. The plant was constructed by the Connecticut Electric Power and Light Company and first operated in 1929 to improve the efficiency of a steam plant located in Devon, Connecticut [32], [33].

From the 1960's through the 1990's, a number of large pumped hydro plants were built to support the growing fleet of nuclear power plants [2], [34]. For example, the Bath County pumped storage plant in the state of Virginia has capacity to operate at 3,003 MW for 10 hours [2]. While pumped hydro plants are efficient and can provide the lowest cost storage on a $/MWh basis, no new pumped hydro plants have been built recently in the United States due to siting issues and the large upfront capitol expense [34]. However, there is still interest, as pumped hydro energy storage is capable of providing long-duration energy capacity with a high power rating. The U.S. Federal Energy Regulatory Commission (FERC) has issued three licenses for proposed pumped hydro projects since 2014 [35].

The only other deployed technology that supports long duration and high power ratings is compressed air energy storage (CAES). The world's first CAES plant was a 290 MW unit that started operation in Huntorf, Germany in 1978 [36]. A second 110 MW system was deployed in McIntosh, Alabama in 1991 [37]. While the early deployments employed a rock cavern for storage, recent efforts have focussed on developing technologies for porous rock to open up more potential sites [38].

One of the first large grid-scale battery system deployments in the United States was the 10 MW/40 MWh lead acid system installed by Southern California Edison in Chino, California in 1988 [39], [40]. At the time, the facility was the world's largest battery plant. The goal of the two-year test program was to demonstrate the benefits and technical feasibility of energy storage operating in a substation environment [39].

The first grid-scale energy storage system demonstration in the United States to enhance small signal stability (e.g., provide damping for an inter-area oscillation) was a 10 MW/30 MJ super conducting magnetic energy storage system installed by the Bonneville Power Administration at a substation in Tacoma, Washington [40]–[42]. The system was designed to provide damping to a 0.35 Hz mode and was first energized on February 16, 1983.

Increased renewable wind generation in the 2000's expanded interest in energy storage technologies. The American Recovery and Reinvestment Act of 2009 (ARRA) provided funding for 16 energy storage demonstration projects, which increased the momentum of the energy storage industry [43], [44]. Twelve of the projects were large grid-connected systems, with a wide range of applications and energy storage technologies. The relatively high costs of storage at the time, combined with multiple potential value streams, started to spur research on stacking benefits to achieve the maximum value out of a deployed system [45], [46].

In 2010, the California legislature passed Assembly Bill No. 2514, which directed the California Public Utilities Commission to determine appropriate targets, if any, for procurement of energy storage by the load-serving entities [47]. Subsequently, in September of 2013, the public utilities commission passed a mandate for 1.3 GW of grid storage to be installed by 2020 [48]. As part of the California energy storage mandate, each load serving entity was required to procure a target amount of energy storage for transmission, distribution, and customer installation. A summary of the targets is listed in Table 4. Similarly, a number of states, including New York and Massachusetts, have announced initiatives and adopted policies directed towards adding a significant amount of energy storage to their electricity infrastructure [49], [50].

TABLE 4. California energy storage mandate targets for utilities (in MW) [48].

Utility	2014	2016	2018	2020	Total
Southern California Edison					
Transmission	50	65	85	110	310
Distribution	30	40	50	65	185
Customer	10	15	25	35	85
Subtotal SCE	**90**	**120**	**160**	**210**	**580**
Pacific Gas and Electric					
Transmission	50	65	85	110	310
Distribution	30	40	50	65	185
Customer	10	15	25	35	85
Subtotal PG&E	**90**	**120**	**160**	**210**	**580**
San Diego Gas & Electric					
Transmission	10	15	22	33	80
Distribution	7	10	15	23	55
Customer	3	5	8	14	30
Subtotal SDG&E	**20**	**30**	**45**	**70**	**165**
Total - all three utilities	**200**	**270**	**365**	**490**	**1,325**

Two regulatory changes put in place by FERC, Order 755 and Order 784, enabled equitable remuneration and participation by all market participants, including energy

storage [51], [52]. Pay-for-performance was mandated by Order 755 [51] in October, 2011. This order required:

> "RTOs and ISOs to compensate frequency regulation resources based on the actual service provided, including a capacity payment that includes the marginal units opportunity costs and a payment for performance that reflects the quantity of frequency regulation service provided by a resource when the resource is accurately following the dispatch signal."

Frequency regulation is the second by second adjustment of generation output power by the independent system operator (ISO) or regional transmission operator (RTO) to maintain the system frequency. Order 784, issued in July 2013, requires public utility transmission providers to consider the speed and accuracy of regulation resources when determining requirements for frequency regulation. This helped open up ancillary service markets for energy storage. Finally, Order 792 issued in November 2013, revised the small generator interconnection procedures (SGIP) and the small generator interconnection agreement (SGIA), enabling energy storage to be put in the same category as small generators [53].

III. ENERGY STORAGE ARCHITECTURES

Energy storage systems are being deployed in a number of configurations. Examples include:

- Large utility owned systems
- Distributed utility owned systems
- Independently owned systems in market areas
- Independently owned systems in vertically integrated utilities
- Small privately owned systems controlled by an aggregator
- Small systems owned and controlled by the aggregator
- Large systems owned by an industrial customer
- Large systems owned by an aggregator to benefit an industrial customer

An example of a large utility-owned system is the 8 MW/32 MWh Tehachapi Wind Energy Storage Plant owned by Southern California Edison [46], shown in Figure 1. In this case, the EMS must interface to other utility systems to coordinate operations with other assets. Since the Tehachapi system is in a market area (California Independent System Operator - CAISO), there would also be a market interface.

Distributed utility owned systems are primarily distribution level assets. An example is the DTE Energy community energy storage (CES) demonstration project in Detroit, Michigan [54], shown in Figure 2. Eighteen 25 kW/50 kWh CES units were deployed, one at the DTE Energy Training and Development Center in Westland, Michigan and seventeen on the TRINITY 9342 distribution circuit near Monroe, Michigan. The 25 kW/50 kWh lithium ion systems were located in a below ground vault, as shown in Figure 2, with the inverter mounted on the vault cover [44]. In this case, the EMS must interface to other utility systems to coordinate operations with other assets.

FIGURE 1. Tehachapi wind energy storage plant, Tehachapi, CA [44].

FIGURE 2. DTE CES system installation, Detroit, MI [44].

In any case, there is a supervisory controller, typically referred to as an EMS, that dispatches one or more energy storage systems. An overview is illustrated in Figure 3. The ownership model, combined with the regulatory structure, greatly impacts the architecture of the EMS. The interfaces to an EMS can include the market, the customer, and the utility, in addition to each storage system.

A typical energy management architecture is presented in Figure 4. At the top is the application/market level, which includes the customer, market, and utility interfaces. The EMS is responsible for optimal and safe operation of the energy storage systems. The EMS system dispatches each of the storage systems. Depending on the application, the EMS may have a component co-located with the energy storage system. In a highly centralized architecture, the EMS provides each system with set points for real and reactive power. In a highly decentralized architecture, the majority of the EMS computations are calculated locally.

The power conversion system (PCS) is responsible for the grid electrical interface and managing power flows. The PCS receives commands from the EMS

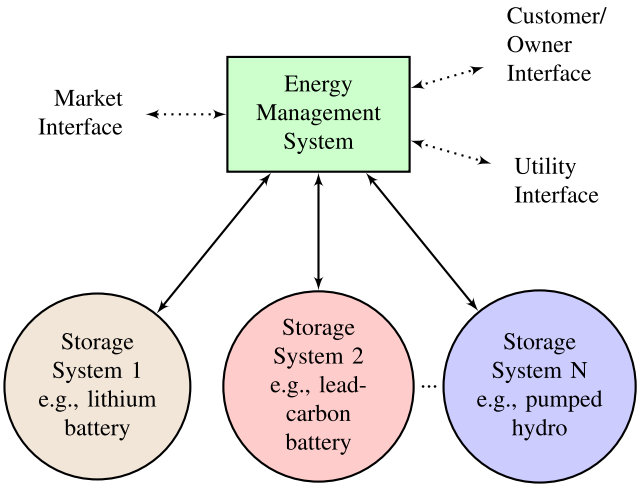

FIGURE 3. Energy management system overview.

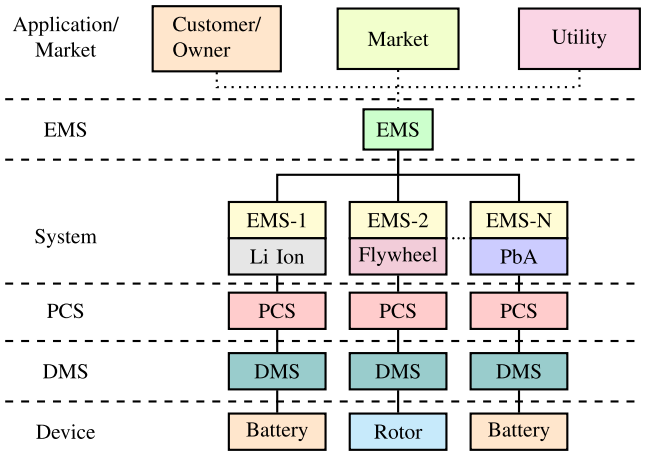

FIGURE 4. Energy management system architecture.

and interfaces to a device management system (DMS). The DMS is responsible for the safe operation of the storage device. Battery-based storage systems typically employ a BMS that is responsible for monitoring and maintaining safe, optimal operation of each battery in the system [19]. For battery based systems, the DMS is often referred to as the BMS.

In practice, it is common for the subsystems of an energy storage system to be made by different manufacturers. Therefore, one of the functions of the EMS is to coordinate their operations. Figure 5 shows a modular EMS dataflow architecture where the subsystems communicate with each other to exchange operating data, including measurements and system states. In many cases, there is not a strict hierarchical organization. For example, Modbus/TCP can be configured where the communications interface is the master, and the DMS, PCS, EMS, and user interface are slaves.

A. ENERGY STORAGE DEVICE MANAGEMENT SYSTEM (DMS)

The DMS is responsible for: 1) Ensuring safe operation of the device; 2) Monitoring and estimating the state of the system;

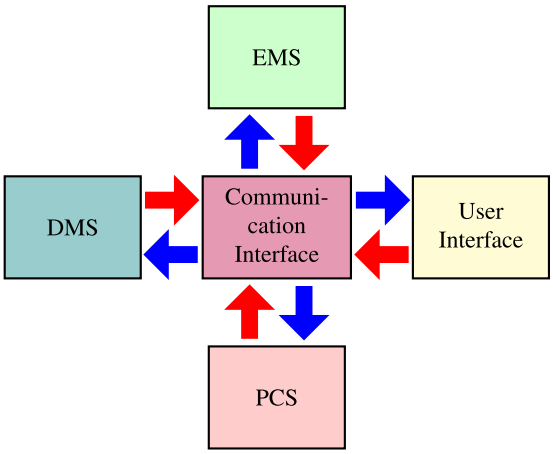

FIGURE 5. Energy storage dataflow architecture.

and 3) Technology specific functions. These DMS functions are designed to maintain safe operation and high performance of the storage device as well as to provide operating data to the EMS and PCS. Information is typically shared among the DMS functions. For example, the state of charge and state estimates are often utilized by all functions. Effectively ensuring safe operation of the device requires access to the state of charge and system state. Likewise, technology specific functions often require this information. The DMS functions are described in more detail below.

1) ENSURING SAFE OPERATION OF THE ENERGY STORAGE DEVICE

Grid systems are capable of storing a significant amount of energy. Therefore, safety mechanisms are required to ensure safe operation of the system. Safety mechanisms can be classified as either active or passive.

Active safety protection systems are used to prevent undesirable working conditions. These include overcharge, overdischarge and overtemperature [55], [56], which significantly reduce the life of the device. For electrochemical systems, this mechanism will disconnect and isolate the string or cell if the voltage, current, or temperature exceed the acceptable operating range. If the rotor speed of a flywheel exceeds the safe operating range, it will be taken off-line. In many cases, the voltage range is predetermined based on the storage technology. The voltage range of a Li-ion battery cell is typically between 2.5V and 4.2V [57]–[59]. Current limits are calculated based on the device state, typically temperature and state of charge. The charge current for a Li-ion cell should be reduced at temperatures below 5°C, and no charging is allowed at temperatures below freezing [56]. Adaptive and predictive approaches have been proposed to maintain safe operation of energy storage devices [60]–[62].

Passive safety protection systems are used to minimize the damage to the device and to the environment in worst-case scenarios. Examples include short-circuits, thermal

runaway, and hazardous chemical leakage. To comply with the current safety codes and standards [63], [64], most energy storage devices are designed and manufactured considering certain types of abuse. Examples include short circuits, abnormal charge/discharge, shock and vibration [65], [66]. Energy storage devices are typically protected against short-circuit currents using fuses and circuit breakers. Thermal isolation of electrochemical cells and packs is often employed to prevent the propagation of thermal runaway [65]. Most batteries include pressure release systems to prevent over-pressure. Vanadium redox flow batteries (VRFB) are required to be self-contained in order to prevent the leakage of the electrolyte into the environment [67]. Enclosures for flywheels are often reinforced and located underground to contain the destructive kinetic energy released by a catastrophic failure [68].

2) MONITORING AND ESTIMATING THE STATE OF THE SYSTEM

In large-scale energy storage systems, multiple storage modules are combined to meet the required energy capacity. Each module is composed of multiple cells. The DMS reads measurements from sensors and meters at the cell and module level (e.g., voltages, currents and temperatures). This data is used to estimate the state variables that cannot be measured directly. The principal states of an energy storage device are described as follows:

The state of charge (SOC) is the available capacity remaining in the device while cycling. In a small number of energy storage systems, the SOC can be measured directly, but in general the SOC can only be estimated through other measurable quantities. For instance, the SOC of a pumped hydro plant can be determined directly from the reservoir level. The SOC of a Li-ion battery, however, can only be estimated and, therefore, cannot be known precisely. The quantities needed for estimation of the SOC differ for various energy storage technologies. Table 5 summarizes the required quantities for several common storage technologies. For example, the SOC of a VRFB can be calculated based on the open-circuit voltage, which is measured through a reference open cell [69], [70]. The SOC of a flywheel can be calculated from its rotor speed and moment of inertia [71], [72]. The SOC of an ultra-capacitor can be estimated from its voltage and impedance captured from experimental data [73], [74]. The SOC of an electrochemical battery can be modeled as a function of terminal voltage, current profile, temperature, and battery age [75]–[78]. These models can vary widely in terms of complexity [19], [79]. In some cases, the SOC can be estimated using a simple model. In other cases, a more sophisticated model may be required, but there is a trade-off between accuracy and computational cost. A simple model is easy to develop and implement but might lead to large errors, whereas a more sophisticated model would provide better accuracy at the expense of higher computational requirements and more difficulty in development and implementation.

TABLE 5. Measurable quantities for SOC calculation.

Technology	Measurable quantities for SOC calculation
Electrochemical batteries	Voltage, current, temperature, age
VRFB	Voltage, temperature, electrolyte concentration
Ultracapacitors	Voltage, capacitance/impedance, temperature
Flywheels	Rotor speed, moment of inertia
Pumped Hydro	Reservoir level
CAES	Pressure, volume, temperature, discharge profile
SMES	Current, inductance

The state of health (SOH) is the present condition of the device compared to its ideal condition. The SOH of an electrochemical cell can be estimated from the ratio of its current capacity to its rated capacity. The most straightforward method for estimating SOH of batteries is to measure the impedance, as it is generally proportional to the capacity loss [80]–[82]. In many cases, this method has high error when the capacity loss and impedance are not well correlated. Model-based methods [83]–[86] and data-driven methods [87]–[89] can be employed to provide more accurate estimation.

3) TECHNOLOGY SPECIFIC FUNCTIONS

Various technologies require technology specific DMS functions. For VRFBs, electrolyte rebalancing between the two half-cells is important to prevent differential ion transfer across the membrane and side reactions [90]. The electrolyte imbalance is often detected by comparing the SOC of both half-cells. Once the electrolyte imbalance is quantified, the chemical reductant can be added to the positive electrolyte to balance the oxidation states [90], [91].

For multi-cell battery packs, unequal cell voltages increase the risk of overcharge/undercharge. To prevent these problems, the DMS must monitor and equalize the battery cell voltages. There are two classes of cell equalization methods: passive and active balancing [92], [93]. The passive balancing method includes two steps [94]: 1) fully charge the battery pack, and 2) remove the excess charge from the cells with highest voltages through passive resistors until their voltages reduce to a reference value. This method is cost effective. However, its main drawback is that if the cooling system cannot effectively dissipate the heat from the passive resistors, it increases the cell temperature thereby reducing the battery life. In the active cell balancing method, charge is transferred from higher voltage cells to lower voltage cells [93], [95]. Switched capacitors, inductors/transformers and power electronics (converters) can be utilized to redistribute the charge between cells [93], [96], [97]. The advantage of this method is that it can effectively reduce the heat loss during the balancing process. However, it involves much more complicated controls and increases the instrumentation cost [93], [98].

B. POWER CONVERSION SYSTEM

With the exception of pumped hydro and compressed air, the majority of energy storage devices employ a direct current (DC) interface. Therefore, a PCS is required to integrate with the alternating current (AC) power grid. The purpose of the PCS is to provide bi-directional conversion and electrical isolation [100].

Several common power conversion architectures are illustrated in Figure 6. A single stage converter has a high efficiency. However, the DC voltage must be greater than 1.5 times the AC RMS voltage [99]. This results in a constraint on the minimum battery string voltage. The multi-stage converter goes from the storage device voltage to an intermediate DC voltage and then converts to AC. This provides more flexibility in the DC voltage range of the storage device at the expense of increased conversion losses and additional hardware costs [99]. A multi-port, multi-stage inverter enables energy storage to interface with solar and other DC sources sharing a common DC bus. When storage is interfaced with PV generation, sharing a common DC bus is more efficient than coupling at the AC grid. A similar architecture is employed to interface to multiple independent battery strings, with the option to include redundancy.

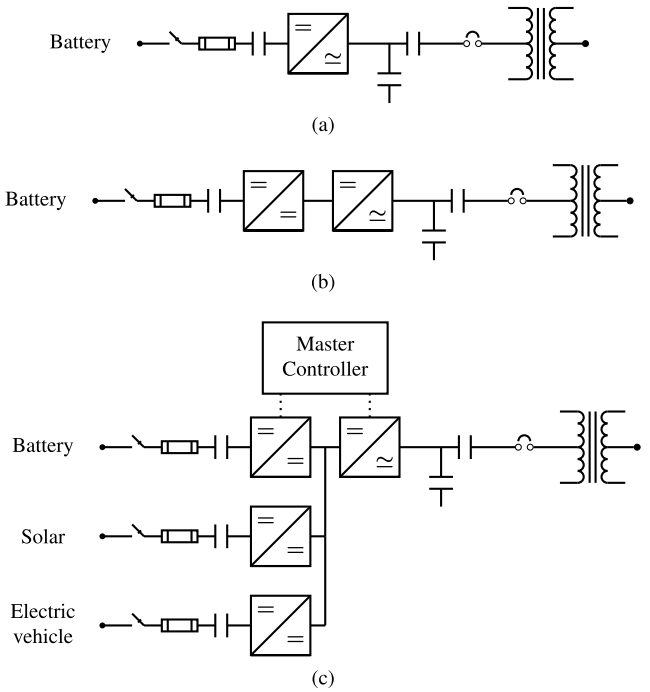

FIGURE 6. PCS architectures [99]. (a) Single stage converter. (b) Multi-stage converter. (c) Multi-port, multi-stage converter.

The PCS management system includes two levels of control [101]: primary and secondary. The secondary control receives power commands (e.g., real and reactive power) from the EMS and the energy storage states (e.g., SOC and temperature) from the DMS [101], [102]. The primary control includes the module level controllers that generate the drive signals for the power converters given the operating mode and the state of the system. The following sections describe the operation of the primary and secondary control in more detail.

1) SECONDARY CONTROL

The secondary control performs the high level management that determines the operating mode for each of the power converters. This is represented by the master controller in Figure 6(c). The three most common modes are: *charging*, *discharging*, and *standby*. These modes are summarized below.

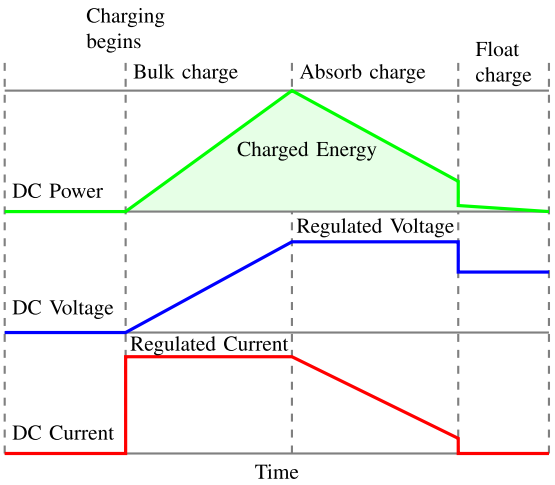

FIGURE 7. Battery 3-stage charging (bulk charge, absorb charge, and float charge).

Charging Mode: This mode occurs when the EMS commands the energy storage device to charge. This mode can include a power level, in which case the charge current is controlled to deliver the commanded power. Otherwise, depending on the SOC of the device, a different charging strategy is selected. Figure 7 shows a 3-stage charging scheme for batteries. The three strategies are:

1) Bulk charge (current control) - used for fast charging when the SOC is low
2) Absorb charge (voltage control) - used to prevent overcharging the battery when the SOC is higher than a certain level
3) Float charge (voltage control) - used when the battery is close to fully charged

This charging scheme can also be applied to ultra-capacitors. The charging time for an ultra-capacitor is much shorter compared to a battery because a much higher current can be tolerated during the bulk charge stage (see Figure 7) [103]–[105]. Similarly, the charging scheme for flywheels includes [34]:

1) Torque control mode (bulk charge)
2) Speed control mode (absorb charge)
3) Power control mode

Discharging Mode: This mode occurs when the EMS commands the energy storage device to discharge. In this mode,

the discharge current is controlled to deliver the commanded power. Two factors that the EMS must take into consideration are: (1) the energy capacity of an electrochemical battery decreases at higher discharge current [106], [107]; and (2) a minimum SOC is often required during discharge to increase cycle life [108], [109].

Standby Mode: The system typically enters standby mode at the conclusion of charging when the maximum SOC limit has been reached. In this mode, the energy storage device is still connected to the system but is not significantly charging or discharging. For an electrochemical battery, float charge might be used to compensate for the self discharge. For a flywheel, a small charge current is used to maintain its nominal speed [110].

For most applications, the above basic operating modes are sufficient to fulfill the EMS commands. However, there has been a push to incorporate advanced inverter functions within the PCS, primarily to enable increased penetrations of distributed solar generation [111]–[115]. Examples of these functions include:

- volt-var (voltage support)
- volt-watt
- constant power factor
- dynamic reactive current
- peak power limiting
- voltage ride-through

Depending on the evolution of these capabilities, some grid control functions may reside in the PCS secondary control going forward.

After the operating mode is specified by the secondary control, control references are calculated and passed to the primary controller.

2) PRIMARY CONTROL

Power electronics enable connection of energy storage systems to the grid, and several topologies are available [116]. Topologies can be classified as transformer based or transformerless depending on the requirement for a coupling transformer. The transformerless topologies include series connection of semiconductors or series connection of submodules (i.e., cascaded H-Bridge converters or modular multilevel converters). The control objective for the primary control is typically charge control, voltage control, current control, or voltage/current control [117], [118].

The most common approach for primary control of a PCS is classic Proportional-Integral (PI) control, although there are several applications of Model Predictive Control (MPC) for power electronics [119]. PI control has been used, for instance, in a modular PCS for a Zinc-Bromine flow battery to regulate both the voltage and current [120]. PI control has also been used for primary control of flywheels [121]–[123] and particularly in wind energy applications [71], [124]. Other examples of primary control approaches include adaptive droop control [125] and the use of MPC for secondary control and hysteresis control for primary control of hybrid power sources [126].

C. COMMUNICATION INTERFACE

Communication between different subsystems is essential for the EMS to coordinate operations. In order to exchange data effectively, each subsystem must be equipped with a communication interface. Basic communication structures for an energy storage system can be found in current standards such as IEC61850-7-420 [127] and MESA [128]. The MESA architecture is illustrated in Figure 8. In practice, commercial systems often follow standardized communication protocols. Modbus/TCP is commonly used in a large number of devices in today's market because of its simplicity and flexibility [129]. Each device equipped with Modbus provides a data register map where each data point is associated with its address. The data register maps can be shared among devices/systems, thereby allowing data exchange between them. DNP3 (Distributed Network Protocol) is more efficient and robust than Modbus. DNP3 plays an important part in modern SCADA systems, which are widely used in power systems [130]. In many cases, the subsystems/devices utilize different communication protocols. To overcome this issue, a software platform that is capable of communicating with a wide range of devices/systems with different protocols is required. An example of such a software platform is VOLTTRON [131], [132].

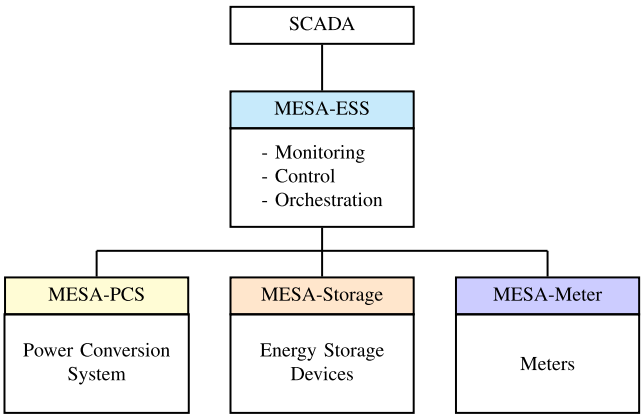

FIGURE 8. MESA communication basic structure [128].

IV. ENERGY APPLICATIONS

Energy applications typically involve long discharge/charge cycles, often lasting more than several hours. In many cases, the design of the system includes a high capacity (MWh) rating to enable the long discharge times at maximum power. Arbitrage has long been proposed as a potential value stream for energy storage [133]. Interest in renewable energy time shift is growing with increased penetrations of behind-the-meter solar in places like California. Demand charge reduction is often a viable strategy for large industrial customers. Time-of-use charge reduction is the same as arbitrage, except the prices are set by the utility. With an aging energy infrastructure and steadily increasing demand growth, transmission and distribution (T&D) upgrade deferral represents a very large potential benefit from energy storage. Another energy

storage application is grid resiliency. The need for improved grid resiliency has been demonstrated by recent events like Hurricane Katrina in New Orleans and Hurricane Sandy in the Northeastern United States.

A. ARBITRAGE

In electricity markets, there are usually diurnal price swings that correspond to times of high demand. Energy arbitrage refers to purchasing (charging) when prices are low and selling (discharging) when prices are high [134]. Figure 9 illustrates typical price swings. The locational marginal price (LMP) in the ISO-NE day-ahead energy market for the Sterling, Massachusetts load node are shown for two different days. On March 23, 2017, there are two peaks. One in the morning as everyone gets up and prepares for the day, and another in the evening as everyone gets home for dinner. On July 14, 2016, there is a peak in the late afternoon from increased air conditioning that combines with the dinner time peak. The number of arbitrage opportunities per day is a function of the number of peaks. The potential revenue is a function of the shape of the peak relative to the trough, as well as the round trip efficiency, η_c, of the energy storage system.

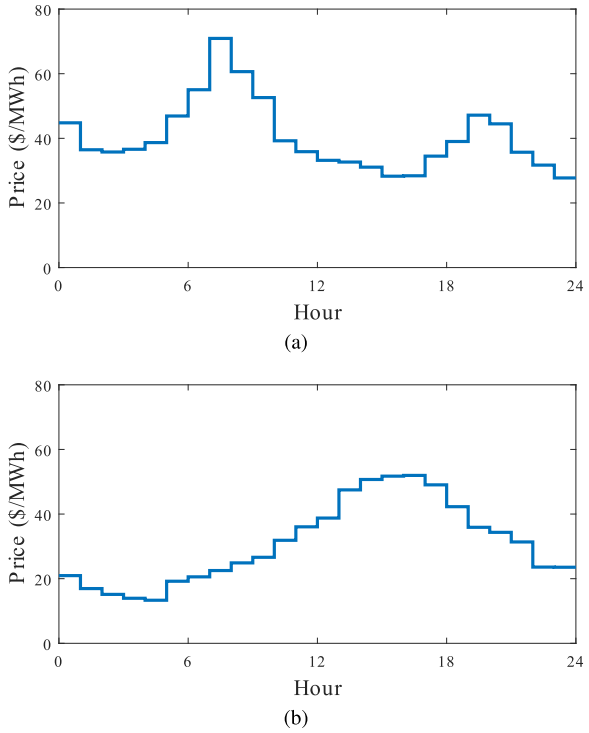

FIGURE 9. Examples of typical variations in day-ahead market energy prices. (a) Day ahead LMP for ISO-NE node 4476 (LD.STERLING13.8), March 23, 2017. (b) Day ahead LMP for ISO-NE node 4476 (LD.STERLING13.8), July 14, 2016.

The arbitrage opportunity is given by:

$$\text{arbitrage opportunity} = q\eta_c LMP_H - qLMP_L \tag{1}$$

where $q\eta_c$ is the discharge quantity (MWh), LMP_H is the average high locational marginal price, q is the charge quantity (MWh), and LMP_L is the average low locational marginal price. In order for arbitrage to be profitable, the ratio of sell/buy price is related to the efficiency by

$$\frac{LMP_H}{LMP_L} \geq \frac{1}{\eta_c} \tag{2}$$

As the round trip efficiency decreases, the difference in prices required to make arbitrage profitable is greater. For example, a system with an 85% round trip efficiency requires that ratio of the high/low prices to be at least 117.6%. Reducing the efficiency to 65% requires that ratio of the high/low prices to be at least 153.8%.

In market areas, compensation for arbitrage is received from participating in the energy markets. In a vertically integrated utility, savings are achieved by more efficient operation of the generation fleet (e.g., flattening of the demand curve with energy storage). The cost savings from arbitrage can be estimated from market data using a Linear Program (LP) optimization [6]–[11]. For a vertically integrated utility, a production cost modeling analysis must be performed to identify the cost savings from different energy storage scenarios [135]–[137].

The dispatch algorithm for arbitrage is typically based on an optimization over a rolling time horizon. Depending on the time increment employed by the market (e.g., 1 hour, 15 minutes, etc.), the device will charge/discharge at the commanded power level over the market time increment. For example, in a day ahead energy market with a 1 hour time increment, the storage system would maintain a constant charge/discharge level for the 1 hour period.

B. RENEWABLE ENERGY TIME SHIFT

Renewable energy time shift is closely related to energy arbitrage. For this benefit, the goal is to shift renewable generation from off-peak to on-peak hours. A classic example is the California "duck curve," illustrated in Figure 10, which has been caused by increasing amounts of PV generation [138]. Figure 10 illustrates a NERC assessment of the expected load, wind, and solar profiles in CAISO projected for January 2020. The first load peak (duck's tail) occurs in the morning as people get up and start preparing for the day. After the sun comes up, there is a decrease in required generation as PV generation increases. The load is at its minimum shortly after lunch (duck's belly) corresponding with the peak PV generation. In late afternoon, as PV resources are declining, load is starting to increase as folks get home from work. This results in a rapid increase in required generation (duck's neck) from 3-6 PM. CAISO introduced a flexible ramping product in the 15- and 5-minute markets on November 1, 2016: Flexible Ramp Up and Flexible Ramp Down. These products are intended to provide the capability to account for uncertainty associated with demand and renewable generation [139]. Energy storage could be used to shift the peak solar energy from midday to late afternoon, mitigating the high ramp rates observed in California.

In market regions without a ramping product, participating in the energy market is the only remuneration mechanism

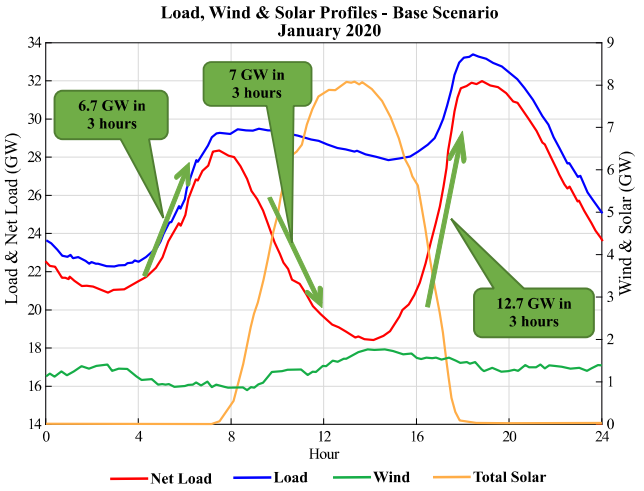

FIGURE 10. Renewable energy time shift example - California 2020 load, wind, and solar profile [140]. Reprinted with permission from NERC.

for providing renewable energy time shift. In general, prices should be lower when large amounts of renewable generation are available. As with arbitrage, the commanded output is calculated based on an optimization over some time horizon, and the power output would typically remain constant over the market time interval.

In a vertically integrated utility, the decision to employ energy storage for renewable energy time shift is based on the reduction in system operating expenses when energy storage is deployed.

C. CUSTOMER DEMAND CHARGE OR TIME-OF-USE CHARGE REDUCTION

Many utilities are switching from fixed-energy price billing models to a combination of demand charges and time-of-use charges. A demand charge is typically based on the maximum rate of consumption ($/kW) over the billing time period (e.g., one month). With demand charges, narrow spikes in demand can significantly increase the electricity bill. Time-of-use charge refers to assigning different rates to various times [141]. This can range from on-peak/off-peak pricing with predefined hours to market rates for each time period.

Mechanisms for achieving the load reductions include chemical energy storage, thermal energy storage, and demand response (DR). Chemical energy storage refers to traditional battery-based systems. Thermal storage includes ice, thermal mass in buildings, and thermal bricks. DR refers to reducing the power draw of various electric appliances or the HVAC system to reduce the overall load.

There are two main demand response programs [142]:

1) INCENTIVE-BASED PROGRAMS

pay participating users for demand reduction, triggered by peak load or system contingencies. These programs include load modification incentives in addition to or separate from electricity prices.

- Direct Load Control (DLC) - utility has remote access to/control of certain appliances/energy loads.
- Interruptible/Curtailable Load - users agree to cut down some portion of their interruptible/curtailable loads when grid reliability is jeopardized and receive incentive discounts on bill.
- Demand bidding and buyback - mainly offered to larger users (1 MW or more), curtail some usage at a specific bid price.
- Emergency Demand Reduction - incentive payments to users in reply to their load reductions (on very short notice) during emergencies. Larger users can provide auxiliary services to the power utility by reducing their demand, behaving as virtual spinning reserve.

2) PRICE-BASED PROGRAMS

provide users different electricity prices at different times.

- Time-of-Use (ToU) pricing - different electricity prices at different time intervals of a day or different seasons of the year. Usually released far in advance and unchanged for long time periods.
- Critical Peak Pricing (CPP) - ToU pricing except for certain days when grid reliability is jeopardized, then normal peak price is replaced by a pre-specified higher rate to reduce users' energy demand. Employed a limited number of hours or days a year.
- Real-Time Pricing (RTP) - (dynamic pricing) Electricity price usually varies at different time intervals of a day (15 min to hour increments). Usually released on an hour-ahead or day-ahead basis. Widely considered one of the most efficient and economic price-based programs.
- Inclining Block Rate (IBR) - two-level rate structures (lower and higher blocks), such that the more electricity a user consumes, the more he/she pays per kWh. Can have hourly/daily/monthly energy consumption thresholds. If distributed over a day, helps to reduce grid's peak-to-average ratio. Widely adopted since 1980s.

The time-of-use charge reduction is the same as arbitrage, except that the rates are from the utility rather than the energy market. Therefore, the commanded output is calculated based on an optimization over some time horizon. For demand charge reduction, the control goal is to make sure that the net load is minimized or never exceeds a predefined value. In this case, the control law just needs to sense the net load and inject power as needed to make sure that the net load remains below the desired value.

D. TRANSMISSION AND DISTRIBUTION UPGRADE DEFERRAL

T&D upgrade deferral can be a very large potential savings/benefit from energy storage. Unfortunately, it is very location specific. In order to realize the benefit, some component of the grid must be exceeding its capacity for a short period of time, and projected load growth makes the problem

worse, ultimately requiring an upgrade. Examples include transmission lines, transformers, and distribution lines that are exceeding their power ratings [143]. By deploying energy storage, the storage can charge when demand is low and then discharge during periods of peak load to keep the assets from exceeding their ratings. In many cases, the energy storage is only called upon several times per year. The required size of the energy storage is a function of the expected load growth and the desired deferral time. The sweet spot for energy storage is a case where there is slow expected load growth and the asset requiring an upgrade is very expensive (e.g., a long transmission line) so that the size of the energy storage remains small relative to the expected benefit.

The economics of T&D deferral for a transmission line example are illustrated in Figure 11 (assuming continuous compounding). In the first scenario, the transmission upgrade occurs immediately. In the second scenario, energy storage enables a deferment of K years for the transmission upgrade. In both scenarios, there are annual costs associated with operation and maintenance (O&M), as well as revenue from transmission tariffs. When the net present value (NPV) of the deferral is greater than the NPV of the upgrade, there is a financial benefit to employing energy storage to defer the cost of the expensive transmission upgrade. If transmission tariff revenue and O&M costs are assumed to be similar for both scenarios, the energy storage investment starts paying off if

$$NPV_{\text{deferral}} - NPV_{\text{upgrade}} \approx -ES_0 - T_K e^{-rK} + T_0 \quad (3)$$

$$ES_0 \leq T_0 - T_K e^{-rK} \quad (4)$$

Furthermore, if the cost of the deferred transmission investment in year K is approximately the same as the cost in year 0 ($T_0 \approx T_K$), then Equation (4) can be expressed as

$$ES_0 \leq T_0 \left(1 - e^{-rK}\right) \quad (5)$$

Related benefits are transmission congestion relief and T&D energy losses. There are costs associated with transmission lines that are operated near capacity in market areas in the form of congestion pricing [144]. Congested transmission lines prevent energy from low-cost generation from meeting all loads. In response, more expensive generation that has a path to the load in the face of the congestion must be employed, raising the price of generation in the constrained area. There are also costs associated with thermal (resistive) losses in the transmission system. These factors can be included in the T&D deferral financial analysis and often make the investment in energy storage more favorable [145].

The commanded output for T&D deferral can be calculated based on an optimization over some time horizon or implemented based on a measurement of the quantity that must be reduced (e.g., transformer loading). In many T&D deferral applications, the energy storage may only be called upon to discharge several hours a year to provide the desired benefit. With proper forecasting, this frees up the device to provide other grid benefits the remainder of the time.

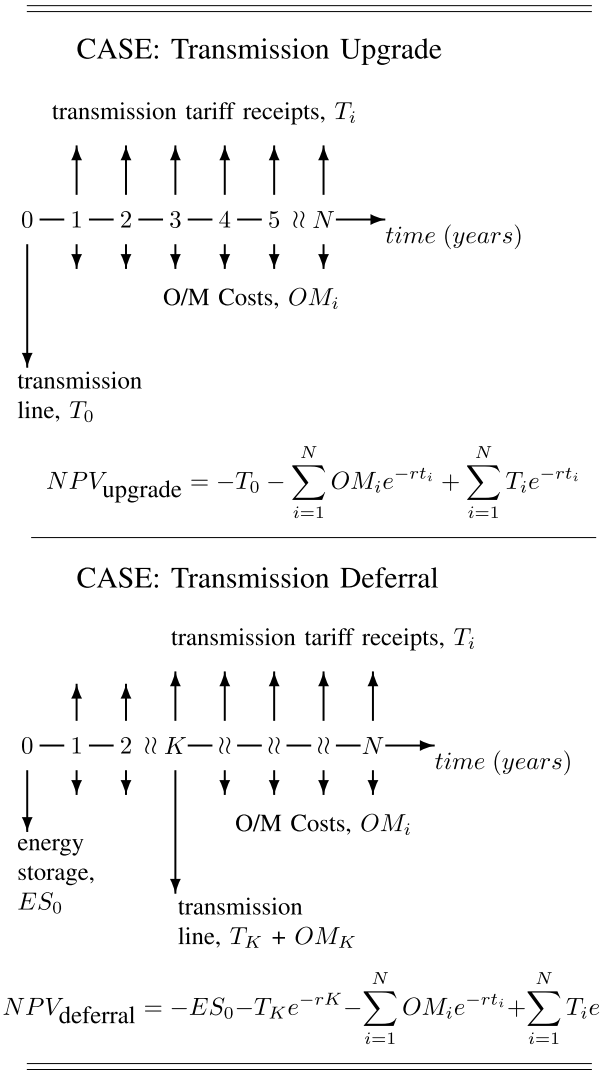

FIGURE 11. Transmission deferral example.

E. GRID RESILIENCY

Severe weather is the leading cause of power outages in the United States. In 2015, severe weather resulted in outages affecting 5,630,618 customers. Data for 2013-2015 is summarized in Table 6. Therefore, grid resiliency is an important application for energy storage. This is especially true for first responders like police and fire departments. Value of Lost Load is defined as the cost of power not delivered ($/kWh or $/MWh). There are two primary methods for estimating interruption costs: indirect and direct [146]. Indirect methods are based on market prices while direct methods typically rely on surveys. The value associated with improved grid resiliency is typically very high, especially if maintaining power to critical loads can prevent the loss of life. Unfortunately, there is no data available specifically for first responders. Data is available in the literature for public administration (small commercial and industrial) [147], which likely underestimates the benefit.

An example of a grid resiliency deployment is the 2 MW, 3.9 MWh system installed by the Sterling Municipal Light

TABLE 6. Percentage of U.S. customers affected by weather related electrical outages [2].

Year	Total Customers Affected	Weather Customers Affected	Percent of Outages from Weather
2013	8,828,313	7,413,172	84.0%
2014	16,850,947	16,788,947	99.6%
2015	6,665,918	6,579,359	98.7%

Department in Sterling, Massachusetts, shown in Figure 12. The lithium ion system was procured primarily to provide back up power for the police, dispatch, and fire service in the case of a weather related outage [10]. Additional applications include reducing payments to the forward capacity market (FCM) and regional network services (RNS). These savings are realized by reducing the monthly (RNS) and annual (FCM) peak loads.

FIGURE 12. Sterling Municipal Light Department 2 MW, 3.9 MWh system for grid resiliency [10].

From a control perspective, the SOC must be maintained at a level that enables operation for the required/expected number of hours that backup power is required, given the expected load. This can be accomplished through the minimum SOC constraint in the EMS.

V. POWER APPLICATIONS

Power applications involve the injection of real and reactive power over short time scales, seconds to minutes, to maintain the stability of the power grid. Frequency regulation, which is the second by second adjustment of output power to maintain the nominal grid frequency, is by far the most common application for large grid-scale energy storage systems. Frequency regulation, voltage support, small signal stability, frequency droop, synthetic inertia, and renewable capacity firming are discussed in the following sections.

A. FREQUENCY REGULATION

The automatic generation signal (AGC) sent to generators for frequency regulation is a function of the frequency error,

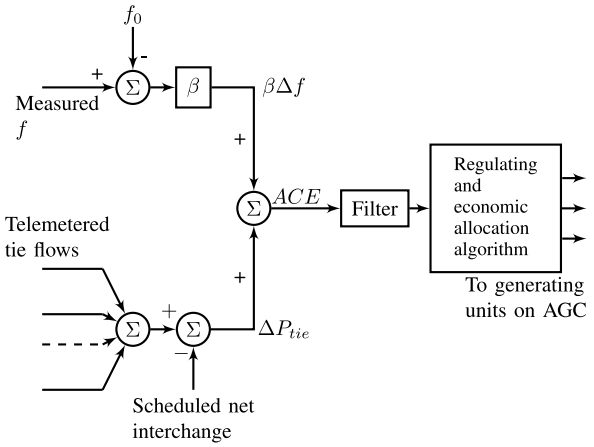

FIGURE 13. Typical AGC control logic for a balancing area [148].

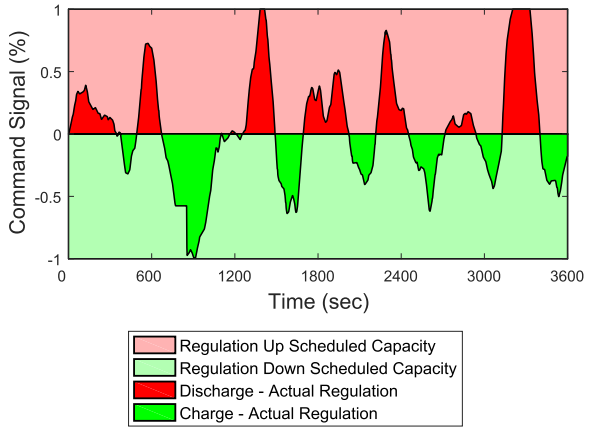

FIGURE 14. Representative regulation command signal (RegD signal from PJM [149]).

measured tie flows, scheduled net interchange, and the bias factor, β, as shown in Figure 13. The bias factor is unique to each balancing area and is a function of the equivalent frequency droop gain and the equivalent damping. The area control error (ACE) is defined as

$$ACE = \Delta P_{tie} + \beta \Delta f \tag{6}$$

where ΔP_{tie} is the difference between the sum of the telemetered tie flows and the scheduled net interchange. Δf is the difference between the measured frequency, f, and the reference frequency, f_0.

Most ISOs transmit an updated AGC signal every 2-4 seconds. Some ISOs have developed a separate signal for fast responding resources like energy storage. An example of such a signal, the RegD signal from PJM, is illustrated in Figure 14. In market areas, products for frequency regulation vary by independent system operator. Some markets provide separate products for regulation up (inject power to the grid) and regulation down (pull power from the grid), while other markets have a single regulation product that assumes bi-directional capability. CAISO and ERCOT are examples of a markets with a separate product for regulation

up and regulation down. PJM is an example of a market with a single regulation product. Different ISOs have formulated varying mechanisms for adhering to FERC Order 755. They incorporate some form of mileage payment that compensates faster responding resources more based on the additional signal mileage. In addition, a performance score based on how accurately the AGC signal was followed is typically incorporated into the formula for remuneration. A survey of ISO practices can be found in [151] and [152].

An example of a flywheel energy storage system designed for providing frequency regulation is the Beacon Power facility at Hazle Township, Pennsylvania shown in Figure 15. The 20 MW/5 MWh plant contains 200 flywheels and can source or sink 20 MW for 15 minutes. Sets of 10 flywheels share a containerized electronics module. Each flywheel stores 25 kWh and has a design life of greater than 100,000 cycles. Each flywheel is installed below grade [44].

FIGURE 15. Beacon flywheel plant at Hazle Township, Pennsylvania [44].

The EMS system must coordinate the market interface for frequency regulation in market areas and make sure that the system has sufficient SOC to follow the AGC signal.

B. VOLTAGE SUPPORT

Energy storage can provide voltage support by modulating real and reactive power. The amount of reactive power that can be provided is limited by the characteristics of the inverter. Oversizing the inverter increases the range of reactive power options as illustrated in Figure 16. The apparent power S is constrained by the following identity:

$$S = \sqrt{P^2 + Q^2} \tag{7}$$

where P is the real power output and Q is the reactive power output. In other words, the apparent power rating S of the inverter must be greater than the real power output P to allow the excess capability for providing reactive power. It is important to note that the storage capacitor inside the inverter must also be suitably oversized to handle the voltage ripple while injecting/absorbing reactive power. Therefore, the reactive power capabilities of smart inverters are often limited when small size capacitors are utilized to reduce the cost and the dimensions of the inverter. This is reflected in the

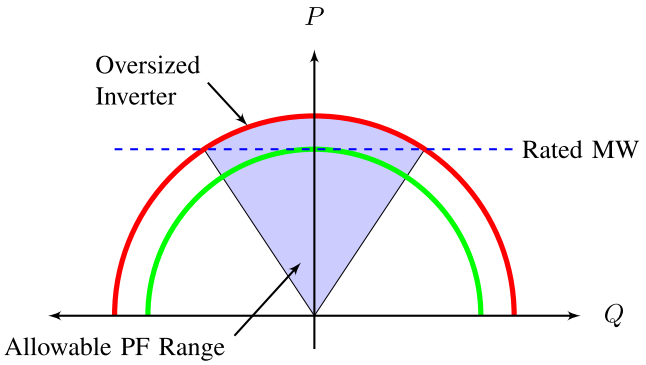

FIGURE 16. Power factor relationship for an oversized inverter.

power factor capabilities of the inverter. Most inverters specify an acceptable power factor (PF) range. For example, if the power factor limit of an inverter is 0.7 (leading or lagging), the inverter can only provide as much reactive power as its real power rating.

There are several different approaches for implementing voltage control. The simplest is to sense the terminal voltage at the point of interconnection, V_t, and then employ a control law with the following structure

$$Q_c = Q_{ref} + K_Q(V_{ref} - V_t) \tag{8}$$

where Q_c is the commanded reactive power, Q_{ref} is the nominal reactive power output, V_{ref} is the desired reference voltage, and K_Q is the reactive power gain. It is common to incorporate a deadband and saturation in the control law, as well as to use a nearby bus for the measured terminal voltage.

Another common reactive power control approach involves the voltage sensitivity matrix [152], [153], $S_Q^{|V|}$, where each term of the matrix is defined as

$$S_Q^{|V|}(i,j) = \frac{\partial V_i}{\partial Q_j} \tag{9}$$

where Q_j represents the reactive power injection at the j^{th} bus, and V_i represents the voltage at the i^{th} bus. The control law is then given by

$$\Delta Q_t^c = \left(S_Q^{|V|}\right)^{-1} \Delta V_t \tag{10}$$

The same approach can be applied to the control of real and reactive power for voltage support.

In practice, PI control is often used to control the voltage response of a Static Compensator [154]. Since an energy storage system is very similar to a Static Compensator, it is likely that this approach will become prevalent for energy storage applications.

Dynamic reactive current is another control scheme proposed for voltage support [155], where the control law is defined as

$$\Delta I_t^{reactive} = -K_{drc} \Delta V_t \tag{11}$$

and K_{drc} is the gain. It is common to incorporate a deadband and saturation with this control law.

Several inverter voltage control functions are being standardized [155], [156] and often apply to energy storage when storage is combined with renewable generation. These include:

- Fixed power factor function (fixed $\cos\phi$)
- Volt-Var function ($Q_t^c = f(V)$)
- Volt-Watt function ($P_t^c = f(V)$)

The fixed power factor function adjusts reactive power to maintain a fixed power factor given a commanded real power level. The Volt-Var function defines a proportional gain equivalent to Equation (8) for calculating the reactive power as a function of the measured voltage. The Volt-Watt defines a proportional gain for calculating the real power as a function of the measured voltage. Both Volt-Var and Volt-Watt typically employ saturation and a deadband.

C. SMALL SIGNAL STABILITY

Small signal stability refers to the stability of the power system in response to small perturbations, where the response can be assumed to be linear. All large power systems are subject to low frequency (0.1-1.0 *Hz*) electromechanical oscillations caused by generator complexes slowly oscillating relative to each other [148], [157], [158]. In the United States, small signal stability is a concern in the Western Interconnection as the 1996 west coast blackout was partially attributed to undamped inter-area oscillations [159].

Given the assumption of a linear response, a state space model can be employed for small signal stability analysis:

$$\dot{x} = Ax + Bu \tag{12}$$

The modes of the system are defined as the eigenvalues of the A-matrix. The mode shape is defined by the right eigenvectors. An illustration of an oscillatory mode in the western North American power grid is shown in Figure 17. The color indicates the phase of the oscillation and the diameter of the circle indicates the amplitude of the oscillation. The bar in the circle indicates the phase angle.

The injection of real power at various locations in the grid based on frequency feedback can be used to damp inter-area oscillations [161], [162]. Energy storage is well suited for this application [163]. There is currently a demonstration project at the Bonneville Power Administration to modulate the power on the Pacific DC Intertie to improve small signal stability. Until this application matures, there are no mechanisms for compensating devices for providing this service. To implement this application, an EMS system has to receive feedback signals (frequency measurements) from remote locations to calculate the control law. Monitoring time delay from the remote measurements is critical, as a long time delay can lead to instability in the control system [164]. Since the oscillation modes are relatively low in frequency, delays up to 100 milliseconds are easily tolerated.

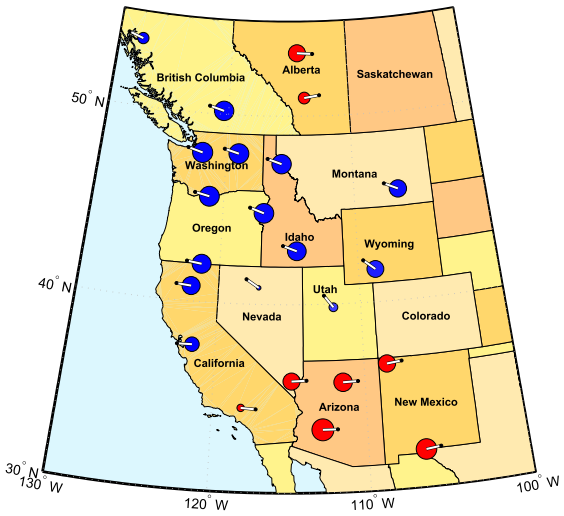

FIGURE 17. North-South Mode B from a 2015 heavy summer Western Electricity Coordinating Council base case simulation [160].

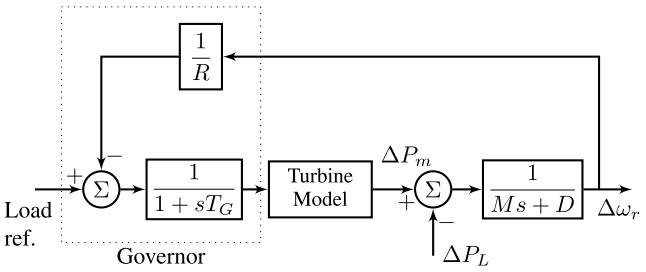

FIGURE 18. Block diagram of a speed governor with droop [148].

D. FREQUENCY DROOP

Frequency droop refers to generator speed control proportional to the speed (frequency) error of the generator. This generator control loop is illustrated in Figure 18. The change in generator mechanical power, ΔP_m, is proportional to the change in rotor speed, $\Delta\omega_r$, times the gain $1/R$. R is typically expressed as a percent:

$$R = \frac{\text{percent speed or frequency change}}{\text{percent power output change}} \times 100 \tag{13}$$

At equilibrium, the mechanical power is given by

$$\Delta P_m = \frac{\Delta\omega_r}{R} \tag{14}$$

because the turbine model has unity gain. Therefore, 5% droop means that a 5% frequency deviation will result in a 100% change in output power.

Generator frequency response service, or frequency droop, is critical for the response of the power system after the loss of a large generator, as illustrated in Figure 19. As the system frequency begins to drop as a result of the loss of generation, the governor response of the generators arrests the drop in system frequency. If fewer generators are providing frequency droop, the frequency nadir will be lower. At some point, this will result in load shedding and ultimately a system breakup. Increased penetrations of renewables, combined

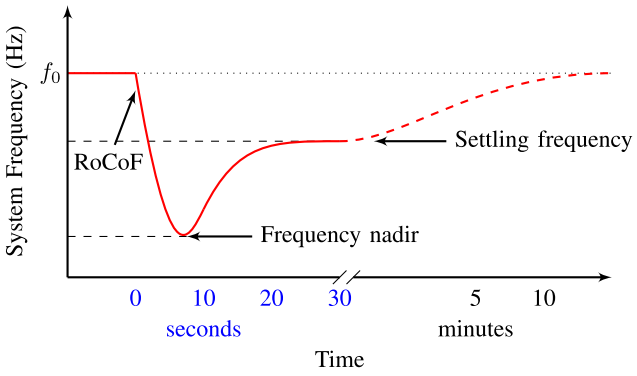

FIGURE 19. System frequency after a loss of generation.

with a lack of rules and compensation regarding generator frequency response service, have led to a decrease in the amount of generator frequency response service. For example, in the Eastern Interconnection in the United States, a lack of frequency response results in a "Lazy L" response [165], where the settling frequency is very close to the frequency nadir.

Inverter based assets like energy storage can emulate the droop characteristics of traditional generation with the following control law:

$$\Delta P = -\frac{1}{R}\Delta f \tag{15}$$

A deadband can be incorporated so that a response only occurs for large frequency excursions.

In the United States, generators are not required to provide a frequency response service, nor are they compensated if they do provide the service. However, FERC issued a notice of inquiry on February 18, 2016 to seek comments on the need for reforms to rules and regulations regarding the provision and compensation of primary frequency response [166]. Options include requiring generating assets to provide a frequency response service as part of an interconnection agreement, combined with a mechanism for fairly compensating the assets for the service. As regulations and market rules evolve, providing frequency response is a potential value stream for energy storage [4], [167].

E. SYNTHETIC INERTIA

The transient response of a typical power system to a loss of generation is illustrated in Figure 19. The initial rate of change of frequency (RoCoF) is a function of how much inertia is in the power system. The more inertia, the slower the initial rate of change in response to a loss of generation. Increasing penetrations of inverter-based renewable generation displace traditional rotating machines, thus reducing the amount of system inertia. A faster initial rate of change usually corresponds with a lower frequency nadir. If the frequency nadir gets too low, loads will trip, and there is a greater chance of a system breakup.

Synthetic inertia refers to injecting power proportional to the rate of change in frequency (which is the second derivative of generator rotor angle). The control law for synthetic inertia, ignoring low-pass filtering, is given by

$$\Delta P = -k_{in}\frac{df}{dt} \tag{16}$$

The units of k_{in} are MW$\cdot s^2$. A deadband can be incorporated if the goal is to only provide synthetic inertia for large frequency excursions.

At this point, there are no mechanisms for compensating resources that provide inertia (conventional or synthetic) to the power system. Some research has been performed investigating benefits of using local frequency versus system frequency, as well as the impact of communications delay on the system frequency measurement [168]. The reduction in inertia from renewable generation is of particular concern for small island grids that already have a small amount of inertia. A study evaluating the benefits of synthetic inertia provided by energy storage for island grids is found in [169]. Curtailed renewable generation is capable of providing synthetic inertia, and methods have been proposed for employing the rotational inertia of wind turbines to provide synthetic inertia [170], [171].

F. RENEWABLE CAPACITY FIRMING

There is inherent variability associated with wind and solar generation. In some areas, limitations are being placed on the maximum allowable ramp rate for renewable generation. For example, the Puerto Rico Electric Power Authority has a minimum technical requirement for PV generation that ramp rates must not exceed 10% of the nameplate capacity per minute [172], [173]. Ramp rate limits have also been imposed for wind generation in Hawaii [174]. An example of solar variability, from a 2.5 MW system located in Sterling, Massachusetts, is illustrated in Figure 20.

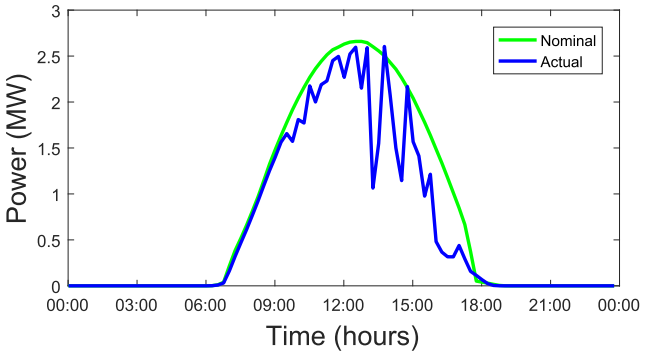

FIGURE 20. Example of solar variability, Sterling, MA, September 28, 2015.

A typical algorithm for ramp rate control is illustrated in Figure 21. The power from the renewable source, P_{gen} is filtered to obtain a signal that meets the ramp rate or other requirements, P_{ref}. Then, the command to the energy storage system is the difference between the renewable generation and the smoothed signal. This ensures that the total power from the storage and renewable generation meets the ramp

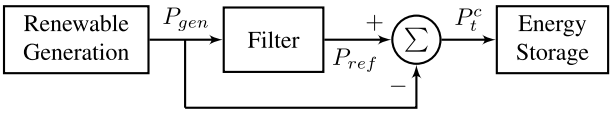

FIGURE 21. Control logic for renewable capacity firming (e.g., ramp rate limiting).

rate requirements. Algorithms for sizing energy storage for solar ramp rate smoothing with various charging scenarios (overnight and daytime) are found in [175]. Results from a demonstration of a PV smoothing algorithm are described in [176].

Depending on the control architecture, the EMS or the renewable generation will be responsible for calculating the power commands to the energy storage system. If the EMS is responsible, it will have to interface to the renewable generation being firmed to receive the P_{gen} feedback signal. The EMS will also have to generate the reference signal.

VI. OPTIMAL OPERATION OF ENERGY STORAGE SYSTEMS

The operation of an energy storage system is often formulated as an optimization problem. Typical goals include maximizing revenue, maximizing grid benefits, or a combination of the two. The energy storage system model is presented in Section VI-A. Different optimization approaches are reviewed in Section VI-B. The optimization problem is formulated for market applications in Section VI-C. The optimization approach for vertically integrated utilities is discussed in Section VI-D. Finally, the operation of behind-the-meter systems is reviewed in Section VI-E.

A. ENERGY STORAGE MODEL

In practice, energy storage modeling is a challenge due to the diversity and complexity of energy storage technologies. A generalized model has the advantage of simplicity and broad applicability; however, it does not precisely capture technology-specific characteristics. On the other hand, a technology-specific model (e.g., Li-ion or VRFB model) is generally more precise. Unfortunately, this type of model is usually based on underlying experimental data of a specific system, and obtaining these experimental data takes time (months or even years) and often requires costly testing facilities.

Energy storage models can be broadly classified into one of the following categories:

- **Dynamic models** - capture the dynamics of the energy conversion process and the power electronics interface to the grid. These models are typically employed for control system design and grid integration studies.
- **Energy flow models** - capture the energy flow, taking into account losses from conversion efficiency and storage efficiency. These models are primarily used for techno-economic analysis and in energy management systems. The model can include time varying parameters, although fixed parameters are more common.
- **Physics-based models** - capture the underlying physical processes involved with the energy storage device. These are often used in SOC estimation and battery management systems.
- **Black box models** - capture the input/output behavior of the storage system. The models are based on experimental data and ignore the underlying physics. Examples include battery degradation models and equivalent circuit models.

Dynamic models are focused on the performance over small time scales, milliseconds to minutes. Often these models ignore SOC and energy related quantities. Energy flow models capture behavior over long periods of time, hours to months. The time step is relatively coarse, minutes to hours, and often corresponds with the market time interval (e.g., hourly day ahead market for energy). Energy flow models provide insight into the charge/discharge profile, which is required in preliminary analysis (e.g., feasibility study, long term planning, selection of the energy storage technology). Since the EMS interfaces to the market, the utility, and the customer/owner, decisions at this level are often based on an energy flow model. At lower levels in the control system, specifically the DMS or BMS, physics-based or dynamic models are often employed. The revenue optimization problem uses energy transactions in the cost function, so it is complimentary with the energy flow model. Physics-based models are highly dependent on the energy storage technology. For mechanical storage, the models include the differential equations that govern the behavior of the underlying energy storage process. For electrochemical storage, the electro-chemical reactions are modeled with partial differential equations. There are many different approaches for developing black box models (e.g., regression, system identification, machine learning, neural networks).

The key parameters that characterize a storage device are [177]:

- **Power Rating** [MW]: the maximum rated power of the storage device (charge and discharge). It is possible to have a different power rating for charging and discharging.
- **Energy Capacity** [MWh]: the amount of energy that can be stored.
- **Efficiency** [percent]: the ratio of the energy discharged by the storage system divided by the energy input into the storage system. Efficiency can be broken down into two components: conversion efficiency and storage efficiency. Conversion efficiency describes the losses encountered when input energy is stored in the system. Storage efficiency describes the time-based losses in a storage system.
- **Ramp Rate** [MW/min or percent nameplate power/min]: the ramp rate describes how quickly a storage system can change its input/output power level.

Example parameter values for several energy storage systems are given in Table 7.

TABLE 7. Example parameter values from projects in [2]

Device	Power Rating [MW]	Energy Capacity [MWh]	Efficiency [%]	Ramp Rate [MW/min]
Li-ion	12	4	90-95	15
Flywheel	20	5	85	300
VRFB	2	8	65-80	120
Pumped hydro	1,119	8,500	70-80	111.9

As mentioned above, EMSs typically employ an energy flow model. The simplest formulation is a discrete linear time-invariant model given by [178]:

$$S_t = \gamma_s S_{t-1} + \gamma_c q_t^R - q_t^D \tag{17}$$

where S_t is the SOC at time t, γ_s is the storage efficiency over one time period, γ_c is the conversion efficiency, q_t^R is the quantity of energy charged over one period, and q_t^D is the quantity of energy discharged over one period. This model assumes constant storage and conversion efficiencies. A fast ramp rate is also assumed so that the energy over each time period is given by

$$\text{total energy} = \text{time period} \times \text{power level} \tag{18}$$

If the ramp rate is slow compared to the time period this approximation does not hold and a model that incorporates ramp rate must be employed.

For the analysis in this paper, we are concerned with the quantity of energy charged or discharged during each time period for each potential activity (e.g. arbitrage, regulation, etc.). For arbitrage, the device will maintain a constant output power over each time period. For regulation, it is assumed that the device is capable of tracking the regulation signal.

The following parameters capture the storage system constraints:

t time period (e.g. one hour)
$\bar{q}^D$ maximum discharged energy in one period (MWh)
$\bar{q}^R$ maximum recharged energy in one period (MWh)
$\bar{S}$ maximum storage capacity (MWh)
$\underline{S}$ minimum storage capacity (MWh)

Since we have assumed that the ramping time is negligible, the maximum quantity that can be sold/discharged in a single period is equivalent to

$$\bar{q}^D = (\text{maximum discharge power level}) \times (\text{time period}) \tag{19}$$

Likewise, the maximum quantity that can be bought/recharged in a single period is equivalent to

$$\bar{q}^R = (\text{maximum recharge power level}) \times (\text{time period}) \tag{20}$$

For a storage device that provides only one service, e.g. arbitrage, there are two decision variables: q_t^D and q_t^R. The decision variables are assumed to be non-negative quantities. Additional constraints include:

$$\underline{S} \le S_t \le \bar{S}, \quad \forall t \tag{21}$$
$$0 \le q_t^R \le \bar{q}^R, \quad \forall t \tag{22}$$
$$0 \le q_t^D \le \bar{q}^D, \quad \forall t \tag{23}$$

For a device that is participating in arbitrage and the regulation market, a few additional quantities must be incorporated into the storage device model. Assuming a separate market for regulation up and regulation down, the additional decision variables are:

q_t^{RU} energy offered into the regulation up market at time t (MWh)
q_t^{RD} energy offered into the regulation up market at time t (MWh)

Once again, the decision variables are assumed to be non-negative quantities. For energy arbitrage, the scheduled and actual quantities are equal. For the regulation market, a resource usually offers a capacity and there is no guarantee that all of the offer will be accepted. Fortunately, since frequency regulation is concerned with the short-term balance of load and generation to maintain system frequency, regulation signals are usually zero mean over longer time periods. This time period varies depending on the market characteristics. For CAISO, the regulation need can have a non-zero mean for up to several hours. On the other hand, the PJM regulation need is zero mean over most 1-hour intervals. A representative regulation command signal is shown in Figure 14.

In order to quantify the change in SOC from participation in the regulation market, it is useful to define the regulation up efficiency γ_{ru} as the fraction of the regulation up reserve capacity that is actually employed in real-time (on average). Similarly, the regulation down efficiency γ_{rd} is the fraction of the regulation down reserve capacity that is actually employed in real-time (on average). For Figure 14 the regulation up/down efficiency is approximately 13%. For some markets where historical regulation data is available, it is possible to calculate γ_{ru} and γ_{rd} at each time step.

The SOC at time t for a device participating in arbitrage and regulation with a separate market for regulation up and regulation down is given by

$$S_t = \gamma_s S_{t-1} + \gamma_c q_t^R - q_t^D + \gamma_c \gamma_{rd} q_t^{RD} - \gamma_{ru} q_t^{RU} \tag{24}$$

subject to the following constraints:

$$\underline{S} \le S_t \le \bar{S}, \quad \forall t \tag{25}$$
$$0 \le q_t^R + q_t^{RD} \le \bar{q}^R, \quad \forall t \tag{26}$$
$$0 \le q_t^D + q_t^{RU} \le \bar{q}^D, \quad \forall t \tag{27}$$

Participating in regulation down provides the opportunity to increase the SOC subject to the regulation down efficiency and the conversion efficiency. Participation in regulation up provides the opportunity to decrease the SOC subject to the regulation up efficiency. The quantities

allocated to regulation up and regulation down reduce the maximum potential quantities allocated to arbitrage subject to the charge/discharge constraints of the device.

For a single (bidirectional) regulation market, the SOC at time t is given by

$$S_t = \gamma_s S_{t-1} + \gamma_c q_t^R - q_t^D + \gamma_c \gamma_{rd} q_t^{REG} - \gamma_{ru} q_t^{REG} \quad (28)$$

where q_t^{REG} is the quantity of regulation that has been accepted by the market. The system is subject to the following constraints:

$$\underline{S} \leq S_t \leq \bar{S}, \quad \forall t \quad (29)$$
$$0 \leq q_t^R + q_t^{REG} \leq \bar{q}^R, \quad \forall t \quad (30)$$
$$0 \leq q_t^D + q_t^{REG} \leq \bar{q}^D, \quad \forall t \quad (31)$$

An alternative formulation of the energy storage model is to define separate efficiencies for charge and discharge using the following definitions,

- γ_r conversion efficiency (fraction of input energy that gets stored) on charge
- γ_d conversion efficiency (fraction of energy that gets output) on discharge
- $\bar{S}^*$ maximum internal energy capacity (MWh)
- $\underline{S}^*$ minumum internal energy capacity (MWh)

The SOC model then becomes

$$S_t^* = \gamma_s S_{t-1}^* + \gamma_r q_t^R - q_t^D / \gamma_d \quad (32)$$

The models in Equation (17) and Equation (32) are equivalent, with the following relationship:

$$S_t = S_t^* \gamma_d \quad (33)$$
$$\bar{S} = \bar{S}^* \gamma_d \quad (34)$$
$$\underline{S} = \underline{S}^* \gamma_d \quad (35)$$
$$\gamma_c = \gamma_d \gamma_r \quad (36)$$

In Equation (32), S_t^* can be understood as the energy stored in the energy storage system. As seen in Equation (33), S_t is the energy available to the load after considering the discharge losses. It is important to note that in percentage terms both of these quantities are equal as $S_t/\bar{S} = S_t^*/\bar{S}^*$. Other variants of the energy storage model include time varying efficiencies. The conversion efficiencies of flow batteries can be strongly dependent on the SOC and charge/discharge power level. For these types of systems, a more accurate model would employ $\gamma_d(S_t^*, q_t^D)$ and $\gamma_r(S_t^*, q_t^R)$ [69]. However, using this model will introduce a nonlinearity making the optimization problem more difficult to solve.

For applications with multiple or stacked benefits, the storage model can be expanded to incorporate the additional activities. When the remuneration from activities are additive, no additional terms are required. For example, if discharging during a time period simultaneously generates revenue from selling electricity in the market, reduces a forward capacity market payment as a result of reducing net load, and reduces a regional network service payment as a result of reducing net load, the multiple benefits are captured in the cost function. Backup power is an example of an activity that is not additive. Energy applied towards delivering backup power is not counted as energy sold into a market. In the case of multiple activities where the remuneration is not additive, the storage model may be updated to include the additional activities:

$$S_t = \gamma_s S_{t-1} + \underbrace{q_t^R \gamma_c - q_t^D}_{\text{energy arbitrage}} + \underbrace{\gamma_c \sum_{i=1}^{N} q_t^{Ri} - \sum_{j=1}^{M} q_t^{Dj}}_{\text{additional activities}} \quad (37)$$

where

- N number of additional recharge activities
- M number of additional discharge activities
- q_t^{Ri} quantity recharged for activity i at time t
- q_t^{Dj} quantity discharged for activity j at time t

B. OPTIMIZATION APPROACHES

The operation of an energy storage system may be posed as an optimization problem where the cost function is defined by a financial metric, a grid benefit metric, or a combination of the two. The constraints are imposed by the energy storage system model and the characteristics of the energy storage system. There are several canonical models that are often applied to decision problems [179].

- Mathematical programming
- Stochastic programming
- Dynamic programming
- Optimal control

Examples of mathematical programming include linear programming (LP) and mixed-integer linear programming (MILP). The problem formulation for each approach is outlined below.

Linear program

$$\begin{aligned} &\text{minimize} && c^\top x \\ &\text{subject to} && Ax \leq b \\ &\text{and} && 0 \leq x \leq \bar{x} \end{aligned}$$

For linear programming, the cost function is a linear combination of the decision variable, x, subject to linear constraints. The decision variables must be greater than or equal to 0 and less than an upper bound $\bar{x}$. The optimal operation of energy storage can be formulated as an LP problem [6]–[10].

Mixed integer linear program

$$\begin{aligned} &\text{minimize} && c^\top x + h^\top y \\ &\text{subject to} && Ax + Gy \leq b \\ &\text{and} && 0 \leq x \leq \bar{x} \\ & && 0 \leq y \leq \bar{y}, \quad y \in \mathbb{Z} \end{aligned}$$

For mixed integer linear programming, a subset of the decision variables y are constrained to be integers. This is useful for problems where there are on/off states associated with the model (e.g., a generator that is on or off). In power systems,

mixed integer programming is often applied to solve the day ahead unit commitment problem for generators, as well as near real-time economic dispatch [180], [181].

A variant of the traditional LP and MILP approaches is robust optimization. Robust optimization typically employs an uncertainty set that includes the worst-case scenarios. By employing a deterministic formulation and modeling the uncertainty via uncertainty sets, the optimization remains computationally tractable for even large systems. A robust unit commitment algorithm for a power system with wind generation and pumped hydro energy storage is presented in [182]. A two stage optimization was employed. The first stage calculates the unit commitment for the day ahead market, while the second stage calculates the real time dispatch for thermal, wind, and hydro generation.

Stochastic programming is employed when randomness must be incorporated into the optimization. The standard formulation is given by [179]

$$\begin{aligned} &\text{minimize} \left(c_t x_t + \sum_{\omega \in \Omega_t} p(\omega) \sum_{t'=t+1}^{t+H} c_{t'}(\omega) x_{t'}(\omega) \right) \\ &\text{over } x_t, (x_{t'}(\omega), t < t' \leq t+H), \forall \omega \in \Omega_t \end{aligned} \tag{38}$$

where ω is called a scenario, which is drawn from a sampled set Ω_t [179]; $p(\omega)$ is the probability of scenario ω; $c_t x_t$ is the realized cost at time t; and $\sum c_{t'}(\omega) x_{t'}(\omega)$ is the total cost across time horizon H when scenario ω occurs. Typically, the stochastic optimization problem is formulated as a two-stage linear program:

- Stage 1 decisions: based on current information
- Stage 2 decisions: made after the random event occurs

Stochastic optimization is often proposed as a method to deal with the intermittence of non-dispatchable renewable generation for power system unit commitment. Results for stochastic optimization of pumped hydro resources combined with wind power are found in [183]. A chance-constrained two-stage stochastic program for unit commitment with uncertain wind power output is presented in [184]. The unit commitment problem with wind generation combined with generic energy storage is formulated in [185].

Dynamic programming is based on the principle of optimality proposed by Bellman [186]:

> "An optimal policy has the property that whenever the initial state and decision are optimal, the remaining decisions must constitute an optimal policy with regard to the state resulting from the first decision."

This enables one to recursively solve the optimization problem working backwards using the Bellman equation [179], which is expressed as:

$$V_t(X_t) = \min_{a \in A} \left(C(X_t, a) + \gamma \sum_{x' \in X} p(x'|X_t, a) V_{t+1}(x') \right) \tag{39}$$

where

X_t	state at time t
a	action in set A
$C(X_t, a)$	cost of being in state X_t and taking action a
γ	fixed discount factor
$p(x'\|x, a)$	probability of transitioning to state $X_{t+1} = x'$ from state $X_t = x$ by action a
$V_t(x)$	value of being in the state $X_t = x$ at time t and following the optimal policy from t onward

Dynamic programming has been proposed for optimizing the use of a battery for participating in arbitrage and frequency regulation [187]. Reasonable results were achieved, but 60 Terabytes of disk space was required to store the value functions for all possible states over a one day period. This highlights a disadvantage of the dynamic programming approach. It does not scale well to large state space models. The one step transition matrix is $N \times N \times A$ where N is the number of states and A is the number of actions [179].

The standard formulation for an optimal control problem given a time varying state space system model

$$\dot{x}(t) = A(t)x(t) + B(t)u(t) \tag{40}$$

is to minimize the performance index V defined as [188]

$$\begin{aligned} V(x(t_0), u(\cdot), t_0) = x^\top(T) H x(T) + \\ \int_{t_0}^{T} \left(u^\top(t) R(t) u(t) + x^\top(t) Q(t) x(t) \right) dt \end{aligned} \tag{41}$$

where the $R(t)$ matrix penalizes the input signal $u(t)$ and the $Q(t)$ matrix penalizes the state vector $x(t)$. The matrix H penalizes the final state at time T. The optimal control input is then given by

$$u^*(t) = -R^{-1}(t) B^\top(t) P(t) x(t) \tag{42}$$

where $P(t)$ is derived from the solution of a matrix Riccati equation. A similar result can be obtained for discrete time systems. This approach is often referred to a the Linear Quadratic Regulator (LQR) problem because of the quadratic form of $V(\cdot)$. The LQR formulation assumes that the states are available. If the states are not available, a Linear Quadratic Estimator (LQE), also known as the Kalman-Bucy Filter [188] may be constructed to provide an optimal estimate of the system states.

The performance of an LQR controller for load frequency control using a SMES system is compared to a fuzzy gain scheduling algorithm in [189]. LQR control of a magnetically suspended flywheel is formulated in [190]. An optimal fixed structure control approach for damping inter-area oscillations is presented in [193] and [194]. An LQR controller combined with a Kalman filter for improving power quality with energy storage is proposed in [193]. By including states that represent the harmonic distortion, the controller was able to improve power quality for a wide range of loads, including those with unbalance.

The LQR optimal control formulation is often applied to lower level control loops that can be easily modeled

TABLE 8. Energy storage optimization problem scenarios from [194].

Scenario	Description
A	A stationary problem with heavy-tailed prices, relatively low noise, moderately accurate forecasts and a reasonably fast storage device.
B	A time-dependent problem with daily load patterns, no seasonalities in energy and price, relatively low noise, less accurate forecasts and a very fast storage device.
C	A time-dependent problem with daily load, energy and price patterns, relatively high noise, less accurate forecasts using time series (errors grow with the horizon) and a reasonably fast storage device.
D	A time-dependent problem with daily load, energy and price patterns, relatively low noise, very accurate forecasts and a reasonably fast storage device.
E	Same as **C**, but the forecast errors are stationary over the planning horizon.

with a state space representation. As the model starts to incorporate other power system components like generators, a MILP or stochastic optimization approach must be employed due to the constraints associated with the ON/OFF states of the generators. In the IEEE Transaction on Power Systems literature, two-stage stochastic programming is the most popular approach to handling uncertainty [194]. In practice, the most prevalent approach for identifying the course of action for the energy storage system is to solve a deterministic optimization using a lookahead forecast. This approach also has relatively good performance for most applications, especially if the constraints are updated to account for uncertainty. A study of different optimization approaches found in [194] compared the following classes of optimization policy for an energy storage system under the scenarios summarized in Table 8:

- Policy function approximation (PFA) - analytic functions mapping states to actions
- Cost function approximation with an error correction term (CFA-EC) - parametric modification of cost function
- Value function approximation (VFA) - approximation of the value of being in a downstream state as a result of an action now
- Look ahead, deterministic optimization (LA-DET)
- Look ahead, deterministic optimization with cost function approximation (LA-CFA) via modification of the constraints

The performance of each optimization approach was evaluated for each scenario relative to the optimal posterior solution. The results from [194] are found in Table 9. While the conclusion of the paper was that it is possible to design realistic energy storage scenarios that highlight the strengths of various optimization policies, another observation is that the forecast, combined with a deterministic optimization and adjustment of the constraints tuned to incorporate expected uncertainty (LA-CFA) performed best on average for all of the scenarios, as indicated by the average scores in Table 9.

TABLE 9. Performance of each class of policy on each problem, relative to the optimal posterior solution, from [194].

Problem	PFA	CFA-EC	VFA	LA-DET	LA-CFA
A	**0.959**	0.839	0.936	0.887	0.887
B	0.714	**0.752**	0.712	0.746	0.746
C	0.865	0.590	**0.914**	0.886	0.886
D	0.962	0.749	0.971	**0.997**	0.997
E	0.865	0.590	0.914	0.922	**0.934**
AVG	0.8730	0.7040	0.8894	0.8876	0.8900

The two scenarios where the LA-CFA approach performed the poorest, **B** and **C**, involved less accurate forecasts and nonstationary forecast errors. However, for these two scenarios, the "best" policy was not significantly better (0.752 vs. 0746 and 0.914 vs. 0.886).

Receding horizon control, also known as MPC [195], [196] is a similar approach that utilizes deterministic optimization with a lookahead forecast. MPC involves the solution of a finite horizon optimization problem, subject to the system dynamics and the other system constraints. Given the current values of the states at time t_0 and forecasts of grid conditions such as demand and generation, an MPC algorithm minimizes a performance index (41), which results in an optimal input signal $u^*(t)$ from time $t = t_0$ to $t = T$, as well as corresponding predictions of the future states using the model (40). Every time new state estimates are available, the finite horizon optimization window slides to the current time, and the MPC problem is resolved. This online solution, as feedback of the states becomes available, helps the algorithm perform well even when unmodeled noise or disturbances are present. Another advantage over, for instance, an LQR approach is that MPC can handle constrained optimizations like the LP and MILP problem formulations described above. Furthermore, MPC can accommodate nonlinear models and explicit handling of disturbances, model uncertainty, and measurement noise [197], [198].

Several recent works utilize MPC for managing energy storage systems. An MPC approach for utilizing energy storage to handle uncertain forecasts for renewable energy sources is discussed in [199]. The use of MPC for energy management of microgrids that include energy storage is studied in in [202] and [203]. Both [202] and [203] present MPC approaches for managing PV storage systems, and MPC for using energy storage for power tracking and peak shaving in distribution grids is described in [204]. The dispatchability of distribution feeders using forecast data and MPC of BESS is studied in [205].

C. MARKET APPLICATIONS

In a market area, an energy storage system's potential revenue is limited to the products offered by the market combined with any other agreements that the system may enter into. For example, it is possible for a utility to procure an energy storage system that is located in a market area, but to rate

base some fraction of the storage based on the services that it provides. An example is the Indianapolis Power and Light 20 MW/20 MWh system located at the Harding Street Station [206]. The system provides primary frequency response, which is not a market product offered by the Midcontinent Independent System Operator (MISO). However, the utility plans to rate base the system and to participate in MISO markets contingent on updates to the MISO frequency regulation market.

The goals of the EMS typically include maximizing the benefits of the system as well as safe operation of the system. Depending on the ownership model, maximizing the benefits corresponds to maximizing revenue, maximizing return on investment, or maximizing grid benefit to the ratepayers. In some situations, it can be a combination of the above. In formulating the optimization, activities that occur on a slower time scale or that have a market interface are captured as decision variables in the optimization. Typically, these are energy applications. Examples include arbitrage and frequency regulation (because of the market interface). Activities that occur on a faster time scale, and often at somewhat random times, are better captured in the constraints. Examples include grid resiliency and small signal stability. The SOC range can be adjusted upward to make sure that enough energy is always available to provide backup power. For the small signal stability application, since the output is bidirectional, the maximum SOC would also have to be adjusted downwards. Likewise, the maximum power ratings must be derated to accommodate activities that are captured in the constraints. The constraints can also be modified to provide a buffer in the face of uncertainty. This is equivalent to a cost function approximation [194].

An outline of the steps required to design the EMS are listed below:

1) Identify revenue streams that the device will participate in
2) Identify activities that require decision variables
3) Identify activities that will be captured via constraints
4) Identify the appropriate time horizon, T, for the look ahead
5) Formulate the cost function

For this example, we assume a single market for frequency regulation and that the device is participating in the following activities:

- Arbitrage
- Frequency regulation
- Primary frequency response (frequency droop)
- Grid resiliency (backup power)

The decision variables are the quantities allocated to arbitrage and frequency regulation in each time period. Primary frequency response and grid resiliency will be captured via constraints. The constraints for an energy storage system are developed using the SOC model.

$$S_t = \gamma_s S_{t-1} + \gamma_c q_t^R - q_t^D + \gamma_c \gamma_{rd} q_t^{REG} - \gamma_{ru} q_t^{REG} \tag{43}$$

The decision variables are the quantity of energy to allocate to charge, recharge, and frequency regulation. In vector form, the decision variables x are written as

$$x^\top = \left[q_1^D \cdots q_T^D \;\; q_1^R \cdots q_T^R \;\; q_1^{REG} \cdots q_T^{REG} \right]^\top \tag{44}$$

The constraints on the SOC and energy transactions at time step t are given by

$$\underline{S}_t \le S_t \le \bar{S}_t \tag{45}$$
$$0 \le q_t^R + q_t^{REG} \le \bar{q}_t^R \tag{46}$$
$$0 \le q_t^D + q_t^{REG} \le \bar{q}^D \tag{47}$$
$$\bar{q}_t^R = \bar{q}^R - q^{DROOP} \tag{48}$$
$$\bar{q}_t^D = \bar{q}^D - q^{RES} - q^{DROOP} \tag{49}$$

Note that the discharge constraints include q^{RES} to capture the power level for the resiliency application, as well as q^{DROOP} to make sure that the power headroom is available for primary frequency response. This over estimates the energy required for droop but is necessary to make sure that the power headroom is available. The charge constraint must also be adjusted to incorporate frequency droop since it is a bidirectional service.

When participating in the frequency regulation market, the conservative approach is to make sure that the SOC is adequate to meet any possible contingency. Therefore, at each time step the SOC limits should be adjusted to take into account the characteristics of the frequency regulation AGC signal.

$$\underline{S}_t = \underline{S} + a_0 q_t^{REG} + a_1 \tag{50}$$
$$\bar{S}_t = \bar{S} - b_0 q_t^{REG} - b_1 \tag{51}$$

The terms a_0 and b_0 can be adjusted based on historical data to make sure that the system has sufficient SOC to meet the majority of the frequency regulation commitments. Since grid resiliency is an application, a_1 must be sized to meet the expected reserve requirements. These terms are influenced by the penalties associated with not providing the required service. If the penalty is small and occurs infrequently, decreasing $\{a_0,\ b_0,\ a_1,\ b_1\}$ frees up SOC for other applications (and potential revenue streams). Note that the model assumes that all conversion losses occur on charging. Therefore, it would be consistent with the model to reduce the upper SOC bound by $\gamma_c b_0\, q_t^{REG}$. However, depending on the actual loss mechanisms in the physical system, this might cause problems and result in a case where the system is unable to accept the assigned recharging for frequency regulation.

Assuming an initial SOC $S_0 = 0$, the linear constraint for the SOC and the upper bound associated with the power rating may be expressed as

$$Ax \le b \tag{52}$$

where

$$A = \begin{bmatrix} -A_d & -A_r & -(A_{ru}+A_{rd}) \\ A_d & A_r & A_{ru}+A_{rd} \\ -I & \mathbf{0} & -I \\ I & \mathbf{0} & I \\ \mathbf{0} & -I & -I \\ \mathbf{0} & I & I \end{bmatrix}$$

$$A_d,\ A_r,\ A_{ru},\ A_{rd}, I\ , \mathbf{0}\ \in \mathbb{R}^{TxT} \tag{53}$$

$$b = \begin{bmatrix} -\underline{\mathcal{S}} \\ \bar{\mathcal{S}} \\ \mathbf{0} \\ \bar{\mathcal{Q}}^D \\ \mathbf{0} \\ \bar{\mathcal{Q}}^R \end{bmatrix}, \quad \underline{\mathcal{S}},\ \bar{\mathcal{S}},\ \bar{\mathcal{Q}}^D,\ \bar{\mathcal{Q}}^R, \mathbf{0}\ \in \mathbb{R}^{Tx1} \tag{54}$$

$$x = \left[\, q_1^D \cdots q_T^D\ q_1^R \cdots q_T^R\ q_1^{REG} \cdots q_T^{REG} \,\right]^\top \tag{55}$$

and each matrix is defined as

$$A_d = \begin{bmatrix} -1 & 0 & 0 & \dots & 0 \\ -\gamma_s & -1 & 0 & \dots & 0 \\ -\gamma_s^2 & -\gamma_s & -1 & \dots & 0 \\ \vdots & \vdots & \vdots & \ddots & \vdots \\ -\gamma_s^{T-1} & -\gamma_s^{T-2} & -\gamma_s^{T-3} & \dots & -1 \end{bmatrix} \tag{56}$$

$$A_r = -\gamma_c A_d \tag{57}$$

$$A_{ru} = \gamma_{ru} A_d \tag{58}$$

$$A_{rd} = \gamma_{rd} A_r \tag{59}$$

$$\bar{\mathcal{S}} = \left[\bar{S}_1\ \bar{S}_2\ \cdots \bar{S}_T\right]^\top \tag{60}$$

$$\underline{\mathcal{S}} = \left[\underline{S}_2\ \underline{S}_1\ \cdots \underline{S}_T\right]^\top \tag{61}$$

$$\bar{\mathcal{Q}}^D = \left[\bar{q}_1^D\ \bar{q}_2^D\ \cdots \bar{q}_T^D\right]^\top \tag{62}$$

$$\bar{\mathcal{Q}}^R = \left[\bar{q}_1^R\ \bar{q}_2^R\ \cdots \bar{q}_T^R\right]^\top \tag{63}$$

The tempo at which an optimization must be performed to operate an energy storage system is a function of the market rules and the activities in which the storage system is participating. A timeline for the ISO New England market is illustrated in Figure 22, which is representative of a typical market.

For a typical market-based energy storage system, the optimization would run prior to the day ahead market (DAM) utilizing a forecast over a time horizon (e.g., 24 hours) to identify the quantities to bid into the day ahead energy and regulation markets. After the market results are published for the DAM, the optimization would run again using the DAM results as additional constraints to identify quantities to bid into the real time market (RTM). Then, at each update time interval for the RTM, the optimization would run again. If there is a change of state, like a portion of the system going off line or a SOC violation as a result of an anomalous AGC signal, the optimization would have to be updated. This behavior is illustrated in Figure 23. Before the operating day is over, the process would repeat for the next operating day.

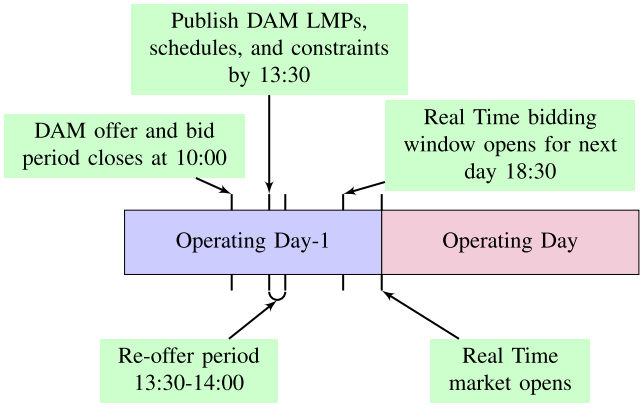

FIGURE 22. ISO New England market timeline [207].

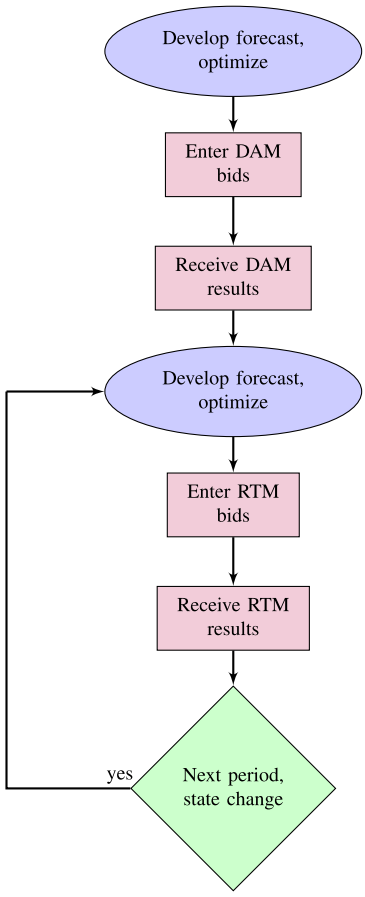

FIGURE 23. Optimization control logic.

D. VERTICALLY INTEGRATED UTILITY APPLICATIONS

A vertically integrated utility is tasked with providing reliable low-cost electricity to customers. The deployment of energy storage is usually a cost saving solution to grid/customer problems. Production cost modeling software is typically employed to optimize the operation of a utility's generation fleet. A production cost modeling tool can be used to identify the cost savings from incorporating energy storage. Examples of potential cost savings include:

- Reduce generation costs by more efficient operation of the conventional generation (e.g., coal, nuclear, natural gas, fuel oil).

- Reduce reserve requirements provided by traditional generation for renewable generation, thus reducing operating costs. For example, storage may enable not running a ''must run'' generator.
- Reduce generation costs associated with providing frequency regulation, and/or reduce the amount of frequency regulation that must be procured.
- Reduce congestion pricing.

The output of a production cost modeling tool is the generator dispatch that yields the lowest system operating costs. The savings from energy storage is the value of storage for that particular scenario. Optimal sizing and placement requires running different scenarios to identify cases that meet benefit/cost ratio requirements or some other metric. In general, there is a diminishing return as the size (power and capacity) of the energy storage is increased. In many cases, the EMS for a storage device in a vertically integrated utility is only required to follow dispatch signals from the centralized dispatch algorithm.

For technical requirements, like meeting a specification for the minimum allowable system frequency after a generator drop, dynamic simulations must be run to identify sizes and locations that meet the technical requirements. Storage must then be compared to other potential solutions. To meet technical requirements, which are often associated with power applications, the EMS must coordinate the various control laws and interact with the centralized dispatching algorithm.

E. BEHIND-THE-METER APPLICATIONS

Optimization algorithms in the EMS can also enable energy storage to be used for behind-the-meter applications. These applications can be broadly referred to as Demand Side Management (DSM) or the implementation of DR techniques (as mentioned in Section IV). The utility goal is to influence the electricity usage of consumers through price or other incentives designed to ensure reliability of the power grid. The goal of the EMS is to minimize the electricity bill or to maximize the grid benefit [142], [208]–[211]. DSM with energy storage has been identified as a crucial element of the future grid [212], [213]. Objectives for DR may include peak shaving, load shifting, or valley filling. In the short-term, DR can impact electricity markets, leading to economic benefits for both the customer and the utility. Resources used for DR include distributed generation, dispatchable loads, and storage devices that can contribute to modifying power supplied by the main grid [209]. In order to make DR less of a burden on the consumer, optimization techniques for automation, monitoring, and control are necessary to manage energy use [209]. These optimization techniques can be designed into an EMS to achieve the objectives of DR while ensuring that storage device constraints, such as maximum capacity, storage efficiency, running cost, charging/discharging rate, etc., are satisfied.

The majority of proposed behind-the-meter optimization algorithms are distributed or at least decentralized. This is because centralized approaches are invasive to users and do not scale well. Next we discuss several optimization approaches to DSM that include stochastic optimization [214], distributed optimization [215], Lyapunov approaches [216], and other techniques spanning the broad fields of advanced control theory and game theory.

1) ADVANCED CONTROL APPROACHES

As mentioned above, MPC is a common and successful advanced control technique that involves the repeated solution of an online optimization problem. This solution includes actions that the EMS should take based on current SOC and forecasts or predictions of conditions in the future, such as power demand and the output from renewable energy sources. Constraints defined in the MPC optimization can ensure that tasks, such as DR, are performed while keeping the SOC as close to a reference value as possible in order to guarantee controllability margins for intervention following a grid contingency [204]. Moreover, multiple DR objectives can be achieved simultaneously, such as power tracking as well as peak shaving [204].

Several different approaches to MPC for DSM have been considered. MPC of PV storage systems is discussed in [202], hierarchical economic MPC for HVAC and building control is described in [217], a distributed MPC approach is given in [218], and hybrid MPC of a residential HVAC system with on-site thermal energy generation and storage is considered in [219]. The advantages of DR for industrial loads are discussed in [220], where an MPC approach coordinates the large discrete power change from the industrial load as well as the fine continuous power change from the energy storage to ensure load following and regulation. In [221], three different MPC architectures (centralized, decentralized, and distributed) are considered for control of residential energy systems with battery storage and are validated using load and generation data from customers in an Australian electricity distribution network.

2) GAME-THEORETIC APPROACHES

Game-theoretic techniques have also been used for optimal DSM [222]–[226]. Several approaches include scheduling of appliances, storage management, and desigining pricing mechanisms [224]. Cooperative game theory can enable cooperative energy exchange in microgrids. Noncooperative game theory can be used to model the interaction between loads and sources in microgrids [224]. Because economic factors, such as markets and pricing, are an essential part of the smart grid, noncooperative games provide a framework that enables designers to optimize pricing strategies as well as consumption schedules that adapt to the nature of the grid. In particular, energy storage systems enable scheduling loads of appliances such as washers and dryers. Much work has been done on computing strategies that minimize the charges for each individual user and maximize the profit for utility companies, while also minimizing the Peak-to-Average Ratio power demand [223]. These types of strategies are computed when considering plug-in hybrid electric vehicles as energy

storage devices in [225] and when large errors are present in renewable energy generation forecasts in [222]. The authors of [227] use an adaptive mechanism for learning the electricity market in their game-theoretic analysis and show reduced peak demands, costs, and carbon emissions.

VII. CONCLUSIONS AND FUTURE DIRECTIONS

Energy storage technology has potential to transform the electricity infrastructure in ways that can fundamentally alter the delivery of energy. While this transformation is at a nascent stage, we need to develop tools that can efficiently use the full range of applications and services that energy storage systems can provide to the electric grid. EMSs play a critical role in the effective utilization of energy storage as a flexible grid asset that can provide multiple grid services and ensure safe operation of energy storage systems.

In this paper, we have made an attempt to provide a comprehensive review of EMSs and optimization tools that are needed for efficient operation of energy storage in the existing grid infrastructure and the grid of the future. Energy storage as an asset class is quite new, and most system operators do not have experience operating energy storage systems. The industry needs robust EMSs and optimization methods that have the flexibility to accommodate multiple storage technologies, new applications, and the ability to operate in evolving market structures. The regulatory environment for energy storage is evolving quickly. This complex regulatory environment, which is a function of location and market structure, makes it difficult to develop generic approaches that meet the needs of a majority of systems. Even with regulatory reforms that make for a level playing field for new technologies including energy storage, storage valuation/optimization continues to be a challenging problem. While there has been significant progress, there are a number of areas requiring additional research:

- **Electrical models that fully reflect the performance and cycle life characteristics of battery systems.** The characteristics of the charge/discharge profile, as well as the SOC profile, can greatly impact the lifetime of electrochemical energy storage systems. Better models are needed so that the EMS optimization can effectively capture the impact to the overall return on investment.
- **Improved optimization approaches for stacked benefits.** The approach presented in this paper yields a very conservative solution for applications that have high power requirements but that occur infrequently. For example, for frequency droop, the maximum expected power rating must be reserved for the whole time interval, which results in an overly conservative SOC constraint. This could also be addressed effectively by designing storage systems with power electronics that have the capability to provide a brief surge.
- **Improved decentralized optimization approaches for grid-scale energy storage.** The approach presented in this paper requires dedicated communication links between the EMS and the storage assets. In many scenarios this may not be reasonable and only limited communications are available. As we look into the distant future, the possibility of decentralized microgrid systems providing the electric power needs of large populations is a distinct possibility. This calls for additional research on energy storage optimization in asynchronous microgrids.
- **Improved grid simulation tools that combine the distribution and transmission network.** It is currently difficult to assess the impact that large quantities of energy storage in the distribution system have on the bulk transmission system. Distribution level modeling tools typically utilize a quasi-static time series simulation and assume a constant grid frequency. In contrast, transmission level simulation tools must "aggregate" distribution level assets but properly model system frequency dynamics. Current modeling tools also are limited in their ability to incorporate the impact of communication networks on the grid and control system performance. Until modeling and simulation capabilities improve, it is difficult to develop, design, and assess various decentralized control techniques.
- **Energy management systems that enable the integration of massive DERs.** Electricity generation in the future is predicted to be much more distributed with a massive number of localized energy resources. Industrial factories, commercial buildings, and residential homes with the ability to generate and store energy, as well as a large number of plug-in electric vehicles, will fundamentally change grid operations. Therefore, enabling energy management systems must be developed to solve this challenge.

Acknowledgment

Sandia National Laboratories is a multi-mission laboratory managed and operated by National Technology and Engineering Solutions of Sandia, LLC., a wholly owned subsidiary of Honeywell International, Inc., for the U.S. Department of Energys National Nuclear Security Administration under contract DE-NA-0003525. The authors would like to thank Meagan Brace for editing the final document, as well as the reviewers who provided very thoughtful feedback.

REFERENCES

[1] North American Electric Reliability Corporation, "2016 long-term reliability assessment," North Amer. Elect. Rel. Corp., Atlanta, GA, USA, Tech. Rep., Dec. 2016. [Online]. Available: https://www.nerc.com
[2] Sandia National Laboratories. (Mar. 2017). *DOE Global Energy Storage Database*. [Online]. Available: https://www.energystorageexchange.org
[3] J. Eyer and G. Corey, "Energy storage for the electricity grid: Benefits and market potential assessment guide," Sandia Nat. Lab., Albuquerque, NM, USA, Tech. Rep. SAND2010-0815, Feb. 2010.
[4] S. Vazquez, S. M. Lukic, E. Galvan, L. G. Franquelo, and J. M. Carrasco, "Energy storage systems for transport and grid applications," *IEEE Trans. Ind. Electron.*, vol. 57, no. 12, pp. 3881–3895, Dec. 2010.

[5] Y. J. Zhang, C. Zhao, W. Tang, and S. H. Low, "Profit maximizing planning and control of battery energy storage systems for primary frequency control," *IEEE Trans. Smart Grid*, doi: 10.1109/TSG.2016.2562672.

[6] R. H. Byrne and C. A. Silva-Monroy, "Estimating the maximum potential revenue for grid connected electricity storage: Arbitrage and the regulation market," Sandia Nat. Lab., Albuquerque, NM, USA, Tech. Rep. SAND2012-3863, Dec. 2012.

[7] R. H. Byrne and C. A. Silva-Monroy, "Potential revenue from electrical energy storage in the Electricity Reliability Council of Texas (ERCOT)," in *Proc. IEEE Power Energy Soc. Gen. Meet. (PESGM)*, Washington, DC, USA, Jul. 2014, pp. 1–5.

[8] R. H. Byrne and C. A. Silva-Monroy, "Potential revenue from electrical energy storage in ERCOT: The impact of location and recent trends," in *Proc. IEEE Power Energy Soc. Gen. Meet. (PESGM)* , Denver, CO, USA, Jul. 2015, pp. 1–5.

[9] R. H. Byrne, R. Concepcion, and C. A. Silva-Monroy, "Potential revenue from electrical energy storage in PJM," in *Proc. IEEE Power Energy Soc. Gen. Meet. (PESGM)* , Boston, MA, USA, Jul. 2016, pp. 1–5.

[10] R. H. Byrne, S. Hamilton, D. R. Borneo, T. Olinsky-Paul, and I. Gyuk, "The value proposition for energy storage at the Sterling Municipal Light Department," in *Proc. IEEE Power Energy Soc. Gen. Meet. (PESGM)*, Chicago, IL, USA, Jul. 2017, pp. 1–5.

[11] T. Nguyen, R. Byrne, R. Conception, and I. Gyuk, "Maximizing revenue from electrical energy storage in MISO energy & frequency regulation markets," in *Proc. IEEE Power Energy Soc. Gen. Meet. (PESGM)*, Chicago, IL, USA, Jul. 2017, pp. 1–5.

[12] H. Khani, M. R. D. Zadeh, and A. H. Hajimiragha, "Transmission congestion relief using privately owned large-scale energy storage systems in a competitive electricity market," *IEEE Trans. Power Syst.*, vol. 31, no. 2, pp. 1449–1458, Mar. 2016.

[13] S. R. Deeba, R. Sharma, T. K. Saha, D. Chakraborty, and A. Thomas, "Evaluation of technical and financial benefits of battery-based energy storage systems in distribution networks," *IET Renew. Power Generat.*, vol. 10, no. 8, pp. 1149–1160, Sep. 2016.

[14] A. Nagarajan and R. Ayyanar, "Design and strategy for the deployment of energy storage systems in a distribution feeder with penetration of renewable resources," *IEEE Trans. Sustain. Energy*, vol. 6, no. 3, pp. 1085–1092, Jul. 2015.

[15] K. W. E. Cheng, B. P. Divakar, H. Wu, D. Kai, and H. F. Ho, "Battery-management system (BMS) and SOC development for electrical vehicles," *IEEE Trans. Veh. Technol.*, vol. 60, no. 1, pp. 76–88, Jan. 2011.

[16] A. Szumanowski and Y. Chang, "Battery management system based on battery nonlinear dynamics modeling," *IEEE Trans. Veh. Technol.*, vol. 57, no. 3, pp. 1425–1432, May 2008.

[17] J. Chatzakis, K. Kalaitzakis, N. C. Voulgaris, and S. N. Manias, "Designing a new generalized battery management system," *IEEE Trans. Ind. Electron.*, vol. 50, no. 5, pp. 990–999, Oct. 2003.

[18] S. Duryea, S. Islam, and W. Lawrance, "A battery management system for stand-alone photovoltaic energy systems," *IEEE Ind. Appl. Mag.*, vol. 7, no. 3, pp. 67–72, Jun. 2001.

[19] M. T. Lawder *et al.*, "Battery energy storage system (BESS) and battery management system (BMS) for grid-scale applications," *Proc. IEEE*, vol. 102, no. 6, pp. 1014–1030, Jun. 2014.

[20] J. Cao, N. Schofield, and A. Emadi, "Battery balancing methods: A comprehensive review," in *Proc. IEEE Veh. Power Propuls. Conf. (VPPC)*, Sep. 2008, pp. 1–6.

[21] D. Pudjianto, C. Ramsay, and G. Strbac, "Virtual power plant and system integration of distributed energy resources," *IET Renew. Power Generat.*, vol. 1, no. 1, pp. 10–16, Mar. 2007.

[22] E. Mashhour and S. M. Moghaddas-Tafreshi, "Bidding strategy of virtual power plant for participating in energy and spinning reserve markets—Part I: Problem formulation," *IEEE Trans. Power Syst.*, vol. 26, no. 2, pp. 949–956, May 2011.

[23] P. Lombardi, M. Powalko, and K. Rudion, "Optimal operation of a virtual power plant," in *Proc. IEEE Power Energy Soc. Gen. Meet. (PESGM)*, Calgary, AB, Canada, Jul. 2009, pp. 1–6.

[24] J. M. Guerrero *et al.*, "Distributed generation: Toward a new energy paradigm," *IEEE Ind. Electron. Mag.*, vol. 4, no. 1, pp. 52–64, Mar. 2010.

[25] N. Hatziargyriou, H. Asano, R. Iravani, and C. Marnay, "MicroGrids," *IEEE Power Energy Mag.*, vol. 5, no. 4, pp. 78–94, Jul./Aug. 2007.

[26] R. H. Lasseter, "MicroGrids," in *Proc. IEEE Power Eng. Soc. Winter Meet.*, vol. 1. New York, NY, USA, Jan. 2002, pp. 305–308.

[27] T. Nguyen, "Optimization in microgrid design and energy management," Ph.D. dissertation, Dept. Elect. Comput. Eng., Missouri Univ. Sci. Technol., Rolla, MO, USA, 2014.

[28] T. T. Gamage, Y. Liu, T. A. Nguyen, X. Qiu, B. M. McMillin, and M. L. Crow, "A novel flow invariants-based approach to microgrid management," *IEEE Trans. Smart Grid*, vol. 6, no. 2, pp. 516–525, Mar. 2015.

[29] X. Wu, X. Hu, S. Moura, X. Yin, and V. Pickert, "Stochastic control of smart home energy management with plug-in electric vehicle battery energy storage and photovoltaic array," *J. Power Sour.*, vol. 333, pp. 203–212, Nov. 2016.

[30] X. Hu, Y. Zou, and Y. Yang, "Greener plug-in hybrid electric vehicles incorporating renewable energy and rapid system optimization," *Energy*, vol. 111, pp. 971–980, Sep. 2016.

[31] A. Ter-Gazarian, *Energy Storage for Power Systems*. London, U.K.: The Institution of Engineering and Technology, 1994.

[32] "A ten-mile storage battery," in *Popular Science Monthly*. New York, NY, USA: Popular Science Publishing Company, Inc., Jul. 1930, p. 60.

[33] American Society of Civil Engineers (ASCE). (2017). *Rocky River Pumped Storage Hydraulic Plant*. [Online]. Available: http://www.asce.org/project/rockyriver-pumped-storage-hydraulic-plant/

[34] F. Díaz-González, A. Sumper, O. Gomis-Bellmunt, *Energy Storage in Power Systems*. Hoboken, NJ, USA: Wiley, 2016.

[35] U.S. Federal Energy Regulatory Commission (FERC). (Jan. 23, 2017). *Pumped Storage Projects*. [Online]. Available: https://www.ferc.gov/industries/hydropower/gen-info/licensing/pump-storage.asp

[36] B. J. Davidson *et al.*, "Large-scale electrical energy storage," *IEE Proc. A-Phys. Sci., Meas. Instrum., Manage. Edu.-Rev.*, vol. 127, no. 6, pp. 345–385, Jul. 1980.

[37] D. R. Mack, "Something new in power technology," *IEEE Potentials*, vol. 12, no. 2, pp. 40–42, Apr. 1993.

[38] A. Narang, "PG&E compressed air energy storage," in *Proc. Elect. Energy Storage Appl. Technol. (EESAT)*, San Diego, CA, USA, Oct. 2011, pp. 215–216.

[39] G. D. Rodriguez, "Operating experience with the Chino 10 MW/40 MWh battery energy storage facility," in *Proc. 24th Intersoc. Energy Convers. Eng. Conf.*, vol. 3. Aug. 1989, pp. 1641–1645.

[40] L. H. Walker, "10-MW GTO converter for battery peaking service," *IEEE Trans. Ind. Appl.*, vol. 26, no. 1, pp. 63–72, Jan. 1990.

[41] H. J. Boenig and J. F. Hauer, "Commissioning tests of the bonneville power administration 30 MJ superconducting magnetic energy storage unit," *IEEE Power Eng. Rev.*, vol. PER-5, no. 2, pp. 32–33, Feb. 1985.

[42] R. Schermer, H. Boenig, M. Henke, R. Turner, and R. Schramm, "Conductor qualification tests for the 30-MJ bonneville power administration SMES coil," *IEEE Trans. Magn.*, vol. MAG-17, no. 1, pp. 356–359, Jan. 1981.

[43] (2015). *American Recovery and Reinvestment Act Overview*. [Online]. Available: http://energy.gov/oe/information-center/recovery-act

[44] D. Bender, R. Byrne, and D. Borneo, "ARRA energy storage demonstration projects: Lessons learned and recommendations," Sandia Nat. Lab., Albuquerque, NM, USA, Tech. Rep. SAND2015-5242, Jun. 2015.

[45] P. Balducci *et al.*, "Assessment of energy storage alternatives in the Puget Sound energy system, volume 1: Financial feasibility analysis," Pacific Northwest Nat. Lab., Richland, WA, USA, Tech. Rep. PNNL-23040, Dec. 2013.

[46] L. Gaillac *et al.*, "Tehachapi wind energy storage project: Description of operational uses, system components, and testing plans," in *Proc. IEEE PES Transmiss. Distrib. Conf. Expo. (T&D)*, Orlando, FL, USA, May 2012, pp. 1–6.

[47] N. Skinner, *California Assembly Bill No. 2514*. Sacramento, CA, USA: State of California, Sep. 2010, ch. 469. [Online]. Available: http://leginfo.legislature.ca.gov/faces/billNavClient.xhtml?bill_id=200920100AB2514

[48] C. Peterman, "Decision adopting energy storage procurement framework and design program," California Public Utilities Commiss. (CPUC), San Francisco, CA, USA, Tech. Rep., Sep. 2013. [Online]. Available: http://docs.cpuc.ca.gov/PublishedDocs/Published/G000/M078/K929/78929853.pdf

[49] New York State Department of Public Services Staff, "Reforming the energy vision—NYS department of public service staff report and proposal," NYSD, White Plains, NY, USA, Tech. Rep. CASE 14-M-0101, 2014.

[50] J. Judson *et al.*, "Massachusetts energy storage initiative," Massachusetts Dept. Energy Resour., Boston, MA, USA, Tech. Rep., 2016. [Online]. Available: https://www.mass.gov/eea/docs/doer/state-of-charge-report.pdf

[51] *Final Rule Order No. 755: Frequency Regulation Compensation in the Organized Wholesale Power Markets*, U.S. Federal Energy Regulatory Commiss., Washington, DC, USA, Oct. 2011.
[52] *Final Rule Order No. 784: Third-Party Provision of Ancillary Services; Accounting and Financial Reporting for New Electric Storage Technologies*, U.S. Federal Energy Regulatory Commiss., Washington, DC, USA, Jul. 2013.
[53] *Final Rule Order No. 792: Small Generator Interconnection Agreements and Procedures*, U.S. Federal Energy Regulatory Commiss., Washington, DC, USA, Nov. 2013.
[54] DTE Energy, "DTE energy advanced implementation of energy storage technologies, technology performance report," DTE Energy, Detroit, MI, USA, Tech. Rep., 2015.
[55] G. Berdichevsky, K. Kelty, J. Straubel, and E. Toomre, "The tesla roadster battery system," *Tesla Motors*, vol. 1, no. 5, pp. 1–5, 2006.
[56] T. Reddy, *Linden's Handbook of Batteries*, 4th ed. New York, Ny, USA: McGraw-Hill, 2010.
[57] LG Chem, "Product specification—Lithium ion battery model: 18650HE2 2500mAh," LG Chem, Seoul, South Korea, Tech. Rep. BCY-PS-HE2-Rev0, 2013.
[58] Samsung SDI Co., Ltd. , "Introduction of INR18650-25R," Samsung SDI Co., Ltd, Gyeonggi-do, South Korea, Tech. Rep., 2013.
[59] Panasonic, "Lithium ion UF103450P," Panasonic, Osaka Prefecture, Japan, Tech. Rep. 13.02.R1, 2013.
[60] S. Mukhopadhyay and F. Zhang, "Adaptive detection of terminal voltage collapses for Li-ion batteries," in *Proc. IEEE 51st Annu. Conf. Decision Control*, Maui, HI, USA, Dec. 2012, pp. 4799–4804.
[61] M. W. Verbrugge, "Adaptive characterization and modeling of electrochemical energy storage devices for hybrid electric vehicle applications," in *Proc. Modeling Numerical Simulations*, 2008, pp. 417–524.
[62] S. Bhide and T. Shim, "Novel predictive electric Li-ion battery model incorporating thermal and rate factor effects," *IEEE Trans. Veh. Technol.*, vol. 60, no. 3, pp. 819–829, Mar. 2011.
[63] *Standard for Lithium Batteries*, Underwriters Laboratories, Northbrook, IL, USA, 2012.
[64] *Secondary Cells and Batteries Containing Alkaline or Other Non-Acid Electrolytes Safety Requirements for Portable Sealed Secondary Cells, and for Batteries Made From Them, for use in Portable Applications*, document IEC 62133-1:2017, Int. Electrotech. Commiss., 2017.
[65] E. Chemali, M. Preindl, P. Malysz, and A. Emadi, "Electrochemical and electrostatic energy storage and management systems for electric drive vehicles: State-of-the-art review and future trends," *IEEE J. Emerg. Sel. Topics Power Electron.*, vol. 4, no. 3, pp. 1117–1134, Sep. 2016.
[66] A. Whitehead, T. Rabbow, M. Trampert, and P. Pokorny, "Critical safety features of the vanadium redox flow battery," *J. Power Sour.*, vol. 351, pp. 1–7, May 2017.
[67] C. J. Rydh, "Environmental assessment of vanadium redox and lead-acid batteries for stationary energy storage," *J. Power Sour.*, vol. 80, no. 1, pp. 21–29, 1999.
[68] D. Bender, "Recommended practices for the safe design and operation of flywheels," Sandia Nat. Lab., Livermore, CA, USA, Tech. Rep. SAND2015-10759, 2015.
[69] T. A. Nguyen, X. Qiu, J. D. Guggenberger, II, M. L. Crow, and A. C. Elmore, "Performance characterization for photovoltaic-vanadium redox battery microgrid systems," *IEEE Trans. Sustain. Energy*, vol. 5, no. 4, pp. 1379–1388, Oct. 2014.
[70] T. A. Nguyen, M. L. Crow, and A. C. Elmore, "Optimal sizing of a vanadium redox battery system for microgrid systems," *IEEE Trans. Sustain. Energy*, vol. 6, no. 3, pp. 729–737, Jul. 2015.
[71] F. Diaz-Gonzalez, F. D. Bianchi, A. Sumper, and O. Gomis-Bellmunt, "Control of a flywheel energy storage system for power smoothing in wind power plants," *IEEE Trans. Energy Convers.*, vol. 29, no. 1, pp. 204–214, Mar. 2014.
[72] F. Faraji *et al.*, "A comprehensive review of flywheel energy storage system technology," *Renew. Sustain. Energy Rev.*, vol. 67, pp. 477–490, Jan. 2017.
[73] L. Zhang, X. Hu, Z. Wang, F. Sun, and D. G. Dorrell, "Experimental impedance investigation of an ultracapacitor at different conditions for electric vehicle applications," *J. Power Sour.*, vol. 287, pp. 129–138, Aug. 2015.
[74] L. Zhang, X. Hu, Z. Wang, F. Sun, and D. G. Dorrell, "Fractional-order modeling and state-of-charge estimation for ultracapacitors," *J. Power Sour.*, vol. 314, pp. 28–34, May 2016.
[75] H. Aung and K. S. Low, "Temperature dependent state-of-charge estimation of lithium ion battery using dual spherical unscented Kalman filter," *IET Power Electron.*, vol. 8, no. 10, pp. 2026–2033, 2015.
[76] C. Zou, C. Manzie, and D. Nešić, "A framework for simplification of PDE-based lithium-ion battery models," *IEEE Trans. Control Syst. Technol.*, vol. 24, no. 5, pp. 1594–1609, Sep. 2016.
[77] C. Zou, C. Manzie, D. Nešić, and A. G. Kallapur, "Multi-time-scale observer design for state-of-charge and state-of-health of a lithium-ion battery," *J. Power Sour.*, vol. 335, pp. 121–130, Dec. 2016.
[78] B. Wang, Z. Liu, S. E. Li, S. J. Moura, and H. Peng, "State-of-charge estimation for lithium-ion batteries based on a nonlinear fractional model," *IEEE Trans. Control Syst. Technol.*, vol. 25, no. 1, pp. 3–11, Jan. 2017.
[79] S. E. Samadani, R. A. Fraser, and M. Fowler, "A review study of methods for lithium-ion battery health monitoring and remaining life estimation in hybrid electric vehicles," Soc. Automotive Eng., Warrendale, PA, USA, SAE Tech. Paper 2012-01-0125, 2012.
[80] F. Huet, "A review of impedance measurements for determination of the state-of-charge or state-of-health of secondary batteries," *J. Power Sour.*, vol. 70, no. 1, pp. 59–69, 1998.
[81] J. Vetter *et al.*, "Ageing mechanisms in lithium-ion batteries," *J. Power Sour.*, vol. 147, no. 1, pp. 269–281, 2005.
[82] H.-F. Yuan and L.-R. Dung, "Offline state-of-health estimation for high-power lithium-ion batteries using three-point impedance extraction method," *IEEE Trans. Veh. Technol.*, vol. 66, no. 3, pp. 2019–2032, Mar. 2017.
[83] T. Kim, W. Qiao, and L. Qu, "Online SOC and SOH estimation for multicell lithium-ion batteries based on an adaptive hybrid battery model and sliding-mode observer," in *Proc. IEEE Energy Convers. Congr. Expo. (ECCE)*, Denver, CO, USA, Sep. 2013, pp. 292–298.
[84] C. Hametner, W. Prochazka, A. Suljanovic, and S. Jakubek, "Model based lithium ion cell ageing data analysis," in *Proc. IEEE Int. Conf. Fuzzy Syst. (FUZZ-IEEE)*, Beijing, China, Jul. 2014, pp. 962–967.
[85] A. Bartlett, J. Marcicki, S. Onori, G. Rizzoni, X. G. Yang, and T. Miller, "Electrochemical model-based state of charge and capacity estimation for a composite electrode lithium-ion battery," *IEEE Trans. Control Syst. Technol.*, vol. 24, no. 2, pp. 384–399, Mar. 2016.
[86] M. Cacciato, G. Nobile, G. Scarcella, and G. Scelba, "Real-time model-based estimation of SOC and SOH for energy storage systems," *IEEE Trans. Power Electron.*, vol. 32, no. 1, pp. 794–803, Jan. 2017.
[87] S. Sarkar, D. K. Jha, A. Ray, and Y. Li, "Dynamic data-driven symbolic causal modeling for battery performance & health monitoring," in *Proc. 18th Int. Conf. Inf. Fusion (Fusion)*, Washington, DC, USA, Jul. 2015, pp. 1395–1402.
[88] C. Hametner, S. Jakubek, and W. Prochazka, "Data-driven design of a cascaded observer for battery state of health estimation," in *Proc. IEEE Int. Conf. Sustain. Energy Technol. (ICSET)*, Hanoi, Vietnam, Nov. 2016, pp. 180–185.
[89] G. You, S. Park, and D. Oh, "Diagnosis of electric vehicle batteries using recurrent neural networks," *IEEE Trans. Ind. Electron.*, vol. 65, no. 6, pp. 4885–4893, Jun. 2017.
[90] S. Corcuera and M. Skyllas-Kazacos, "State-of-charge monitoring and electrolyte rebalancing methods for the vanadium redox flow battery," *Eur. Chem. Bull.*, vol. 1, no. 12, pp. 511–519, 2012.
[91] M Skyllas-Kazacos, "Secondary batteries-flow systems vanadium redox-flow batteries, " in *Encyclopedia of Electrochemical Power Sources*, J. Garche, Ed. New York, NY, USA: Elsevier, 2009, pp. 444–453.
[92] S. W. Moore and P. J. Schneider, "A review of cell equalization methods for lithium ion and lithium polymer battery systems," Soc. Automotive Eng., Warrendale, PA, USA, SAE Tech. Paper 2001-01-0959, 2001.
[93] M. Daowd, N. Omar, P. Van den Bossche, and J. Van Mierlo, "A review of passive and active battery balancing based on MATLAB/Simulink," *Int. Rev. Elect. Eng.*, vol. 6, pp. 2974–2989, Nov. 2011.
[94] N. H. Kutkut and D. M. Divan, "Dynamic equalization techniques for series battery stacks," in *Proc. 18th Int. Telecommun. Energy Conf. (INTELEC)*, 1996, pp. 514–521.
[95] M. Einhorn, W. Roessler, and J. Fleig, "Improved performance of serially connected Li-ion batteries with active cell balancing in electric vehicles," *IEEE Trans. Veh. Technol.*, vol. 60, no. 6, pp. 2448–2457, Jul. 2011.
[96] T. A. Stuart and W. Zhu, "Fast equalization for large lithium ion batteries," *IEEE Aerosp. Electron. Syst. Mag.*, vol. 24, no. 7, pp. 27–31, Jul. 2009.
[97] W. C. Lee, D. Drury, and P. Mellor, "Comparison of passive cell balancing and active cell balancing for automotive batteries," in *Proc. IEEE Veh. Power Propuls. Conf. (VPPC)*, Chicago, IL, USA, Sep. 2011, pp. 1–7.

[98] X. Zhang, P. Liu, and D. Wang, "The design and implementation of smart battery management system balance technology," *J. Converg. Inf. Technol.*, vol. 6, no. 5, pp. 108–116, 2011.
[99] K. Clark, "Power conversion system architectures," in *Proc. Workshop High Megawatt Electron., Technol. Roadmap Increased Power Electron. Grid Appl. Devices*, Gaithersburg, MD, USA, May 2102, pp. 1–17.
[100] B. Zakeri and S. Syri, "Electrical energy storage systems: A comparative life cycle cost analysis," *Renew. Sustain. Energy Rev.*, vol. 42, pp. 569–596, Feb. 2015.
[101] G. Oriti, A. L. Julian, and N. J. Peck, "Power-electronics-based energy management system with storage," *IEEE Trans. Power Electron.*, vol. 31, no. 1, pp. 452–460, Jan. 2016.
[102] J. Xiao, P. Wang, and L. Setyawan, "Multilevel energy management system for hybridization of energy storages in DC microgrids," *IEEE Trans. Smart Grid*, vol. 7, no. 2, pp. 847–856, Feb. 2016.
[103] P. J. Grbovic, P. Delarue, P. L. Moigne, and P. Bartholomeus, "Modeling and control of the ultracapacitor-based regenerative controlled electric drives," *IEEE Trans. Ind. Electron.*, vol. 58, no. 8, pp. 3471–3484, Aug. 2011.
[104] P. P. Mercier and A. P. Chandrakasan, "Rapid wireless capacitor charging using a multi-tapped inductively-coupled secondary coil," *IEEE Trans. Circuits Syst. I, Reg. Papers*, vol. 60, no. 9, pp. 2263–2272, Sep. 2013.
[105] C. Woo-Young, "High-efficiency duty-cycle controlled full-bridge converter for ultracapacitor chargers," *IET Power Electron.*, vol. 9, no. 6, pp. 1111–1119, 2016.
[106] D. Doerffel and S. A. Sharkh, "A critical review of using the Peukert equation for determining the remaining capacity of lead-acid and lithium-ion batteries," *J. Power Sour.*, vol. 155, no. 2, pp. 395–400, 2006.
[107] S. Ioannou, K. Dalamagkidis, E. Stefanakos, K. Valavanis, and P. Wiley, "Runtime, capacity and discharge current relationship for lead acid and lithium batteries," in *Proc. 24th Med. Conf. Control Autom. (MED)*, Athens, Greece, 2016, pp. 46–53.
[108] G. Ning and B. N. Popov, "Cycle life modeling of lithium-ion batteries," *J. Electrochem. Soc.*, vol. 151, no. 10, pp. A1584–A1591, 2004.
[109] G. Ning, R. E. White, and B. N. Popov, "A generalized cycle life model of rechargeable Li-ion batteries," *Electrochim. Acta*, vol. 51, no. 10, pp. 2012–2022, 2006.
[110] H. Gabbar, *Smart Energy Grid Engineering*. San Francisco, CA, USA: Academic, 2016.
[111] W. Sunderman, R. C. Dugan, and J. Smith, "Open source modeling of advanced inverter functions for solar photovoltaic installations," in *Proc. IEEE PES*, Chicago, IL, USA, Apr. 2014, pp. 1–5.
[112] R. Dugan, W. Sunderman, and B. Seal, "Advanced inverter controls for distributed resources," in *Proc. 22nd Int. Conf. Exhib. Elect. Distrib. (CIRED)*, Stockholm, Sweden, Jun. 2013, pp. 1–4.
[113] M. Ammar and G. Joós, "A short-term energy storage system for voltage quality improvement in distributed wind power," *IEEE Trans. Energy Convers.*, vol. 29, no. 4, pp. 997–1007, Dec. 2014.
[114] S.-J. Lee *et al.*, "Coordinated control algorithm for distributed battery energy storage systems for mitigating voltage and frequency deviations," *IEEE Trans. Smart Grid*, vol. 7, no. 3, pp. 1713–1722, May 2016.
[115] E. Serban, M. Ordonez, and C. Pondiche, "Voltage and frequency grid support strategies beyond standards," *IEEE Trans. Power Electron.*, vol. 32, no. 1, pp. 298–309, Jan. 2017.
[116] G. Wang *et al.*, "A review of power electronics for grid connection of utility-scale battery energy storage systems," *IEEE Trans. Sustain. Energy*, vol. 7, no. 4, pp. 1778–1790, Oct. 2016.
[117] D. Pavković, M. Hrgetić, A. Komljenović, and V. Smetko, "Battery current and voltage control system design with charging application," in *Proc. IEEE Conf. Control Appl. (CCA)*, Juan Les Antibes, France, Oct. 2014, pp. 1133–1138.
[118] W. Chen, X. Ruan, H. Yan, and C. K. Tse, "DC/DC conversion systems consisting of multiple converter modules: Stability, control, and experimental verifications," *IEEE Trans. Power Electron.*, vol. 24, no. 6, pp. 1463–1474, Jun. 2009.
[119] S. Vazquez *et al.*, "Model predictive control: A review of its applications in power electronics," *IEEE Ind. Electron. Mag.*, vol. 8, no. 1, pp. 16–31, Mar. 2014.
[120] J.-U. Lim, S.-J. Lee, K.-P. Kang, Y. Cho, and G.-H. Choe, "A modular power conversion system for Zinc-Bromine flow battery based energy storage system," in *Proc. IEEE 2nd Int. Future Energy Electron. Conf. (IFEEC)*, Nov. 2015, pp. 1–5.
[121] H. Akagi and H. Sato, "Control and performance of a doubly-fed induction machine intended for a flywheel energy storage system," *IEEE Trans. Power Electron.*, vol. 17, no. 1, pp. 109–116, Jan. 2002.
[122] H. Silva-Saravia, H. Pulgar-Painemal, and J. M. Mauricio, "Flywheel energy storage model, control and location for improving stability: The Chilean case," *IEEE Trans. Power Syst.*, vol. 32, no. 4, pp. 3111–3119, Jul. 2017.
[123] B. H. Kenny, P. E. Kascak, R. Jansen, T. Dever, and W. Santiago, "Control of a high-speed flywheel system for energy storage in space applications," *IEEE Trans. Ind. Appl.*, vol. 41, no. 4, pp. 1029–1038, Jul. 2005.
[124] R. Sebastián and R. Peña-Alzola, "Control and simulation of a flywheel energy storage for a wind diesel power system," *Int. J. Electr. Power Energy Syst.*, vol. 64, pp. 1049–1056, 2015.
[125] X. Lu, K. Sun, J. M. Guerrero, J. C. Vasquez, and L. Huang, "State-of-charge balance using adaptive droop control for distributed energy storage systems in DC microgrid applications," *IEEE Trans. Ind. Electron.*, vol. 61, no. 6, pp. 2804–2815, Jun. 2014.
[126] R. T. Bambang, A. S. Rohman, C. J. Dronkers, R. Ortega, A. Sasongko, "Energy management of fuel cell/battery/supercapacitor hybrid power sources using model predictive control," *IEEE Trans. Ind. Informat.*, vol. 10, no. 4, pp. 1992–2002, Nov. 2014.
[127] F. M. Cleveland, "IEC 61850-7-420 communications standard for distributed energy resources (DER)," in *Proc. IEEE Power Energy Soc. Gen. Meet.*, Pittsburgh, PA, USA, Jul. 2008, pp. 1–4.
[128] (2017). *MESA—Open Standard for Energy Storage*. [Online]. Available: http://mesastandards.org/mesa-device/
[129] (2017). *MESA—PCS Specification*. [Online]. Available: https://goo.gl/6FRgfP
[130] *IEEE Standard for Exchanging Information Between Networks Implementing IEC 61850 and IEEE Std 1815(TM) [Distributed Network Protocol (DNP3)]*, IEEE Standard 1815.1-2015 (Incorporates IEEE Std 1815.1-2015/Cor 1-2016), Dec. 2016, pp. 1–358.
[131] J. Haack, B. Akyol, N. Tenney, B. Carpenter, R. Pratt, and T. Carroll, "VOLTTRON: An agent platform for integrating electric vehicles and smart grid," in *Proc. Int. Conf. Connected Veh. Expo (ICCVE)*, Las Vegas, NV, USA, Dec. 2013, pp. 81–86.
[132] S. Katipamula, J. Haack, G. Hernandez, B. Akyol, and J. Hagerman, "VOLTTRON: An open-source software platform of the future," *IEEE Electrific. Mag.*, vol. 4, no. 4, pp. 15–22, Dec. 2016.
[133] F. Graves, T. Jenkin, and D. Murphy, "Opportunities for electricity storage in deregulating markets," *Elect. J.*, vol. 12, no. 8, pp. 46–56, 1999.
[134] A. S. A. Awad, J. D. Fuller, T. H. M. EL-Fouly, and M. M. A. Salama, "Impact of energy storage systems on electricity market equilibrium," *IEEE Trans. Sustain. Energy*, vol. 5, no. 3, pp. 875–885, Jul. 2014.
[135] J. Ellison, D. Bhatnagar, and B. Karlson, "Maui energy storage study," Sandia Nat. Lab., Albuquerque, NM, USA, Tech. Rep. SAND2012-10314, Dec. 2012.
[136] J. F. Ellison, D. Bhatnagar, N. Saaman, and C. Jin, "NV energy electricity storage valuation," Sandia Nat. Lab., Albuquerque, NM, USA, Tech. Rep. SAND2013-4902, Jun. 2013.
[137] J. Ellison, D. Bhatnagar, C. Black, and K. Jenkins, "Southern company energy storage study: A study for the DOE energy storage systems program," Sandia Nat. Lab., Albuquerque, NM, Tech. Rep. SAND2013-2251, Mar. 2013.
[138] California Independent System Operator (CAISO). (2016). *What the Duck Curve Tells US About Managing a Green Grid*. [Online]. Available: https://www.caiso.com
[139] California Independent System Operator (CAISO). (2016). *Flexible Ramping Product*. [Online]. Available: https://www.caiso.com
[140] R. W. Cummings, "Energy storage and reliability," in *Proc. Energy Storage Workshop Southwest Public Utility Regulatory Commiss.*, Albuquerque, NM, USA, May 2016, pp. 1–34.
[141] S. Chen, H. A. Love, and C.-C. Liu, "Optimal opt-in residential time-of-use contract based on principal-agent theory," *IEEE Trans. Power Syst.*, vol. 31, no. 6, pp. 4415–4426, Nov. 2016.
[142] R. Deng, Z. Yang, M. Chow, and J. Chen, "A survey on demand response in smart grids: Mathematical models and approaches," *IEEE Trans. Ind. Informat.*, vol. 11, no. 3, pp. 570–582, Jun. 2015.
[143] M. Kleinberg *et al.*, "Energy storage valuation under different storage forms and functions in transmission and distribution applications," *Proc. IEEE*, vol. 102, no. 7, pp. 1073–1083, Jul. 2014.
[144] V. Virasjoki, P. Rocha, A. S. Siddiqui, and A. Salo, "Market impacts of energy storage in a transmission-constrained power system," *IEEE Trans. Power Syst.*, vol. 31, no. 5, pp. 4108–4117, Sep. 2016.
[145] A. Nourai, V. I. Kogan, and C. M. Schafer, "Load leveling reduces T&D line losses," *IEEE Trans. Power Del.*, vol. 23, no. 4, pp. 2168–2173, Oct. 2008.

[146] M. Ligus, "The value of supply security," in *Proc. IEEE 15th Int. Conf. Environ. Electr. Eng. (EEEIC)*, Jun. 2015, pp. 1846–1851.
[147] M. J. Sullivan, M. Mercuriov, and J. Schellenberg, "Estimated value of service reliability for electric utility customers in the United States," Ernest Orlando Lawrence Berkeley Nat. Lab., Berkeley, CA, USA, Tech. Rep. LBNL-2132E, Jun. 2009.
[148] P. Kundur, *Power System Stability and Control*. New York, NY, USA: McGraw-Hill, 1993.
[149] PJM. (2016). *RTO Regulation Signal Data*. [Online]. Available: http://www.pjm.com/markets-and-operations/ancillary-services.aspx
[150] M. Kintner-Meyer, "Regulatory policy and markets for energy storage in North America," *Proc. IEEE*, vol. 102, no. 7, pp. 1065–1072, Jul. 2014.
[151] B. Xu, Y. Dvorkin, D. S. Kirschen, C. A. Silva-Monroy, and J.-P. Watson, "A comparison of policies on the participation of storage in U.S. frequency regulation markets," in *Proc. IEEE Power Energy Soc. Gen. Meet. (PESGM)*, Jul. 2016, pp. 1–5.
[152] A. Samadi, R. Eriksson, L. Söder, B. G. Rawn, and J. C. Boemer, "Coordinated active power-dependent voltage regulation in distribution grids with PV systems," *IEEE Trans. Power Del.*, vol. 29, no. 3, pp. 1454–1464, Jun. 2014.
[153] M. J. Reno, J. E. Quiroz, O. Lavrova, and R. H. Byrne, "Evaluation of communication requirements for voltage regulation control with advanced inverters," in *Proc. North Amer. Power Symp. (NAPS)*, Denver, CO, USA Sep. 2016, pp. 1–6.
[154] P. Rao, M. L. Crow, and Z. Yang, "STATCOM control for power system voltage control applications," *IEEE Trans. Power Del.*, vol. 15, no. 4, pp. 1311–1317, Oct. 2000.
[155] B. Seal and B. Ealey, "Common functions for smart inverters, version 3," Elect. Power Res. Inst., Palo Alto, CA, USA, Tech. Rep. 3002002233, 2014.
[156] M. Kraiczy, A. L. Fakhri, T. Stetz, and M. Braun, "Do it locally: Local voltage support by distributed generation—A management summary," Int. Energy Agency, Paris, France, Tech. Rep. IEA-PVPS T14-08:2017, 2017.
[157] L. Shi, K. Y. Lee, and F. Wu, "Robust ESS-based stabilizer design for damping inter-area oscillations in multimachine power systems," *IEEE Trans. Power Syst.*, vol. 31, no. 2, pp. 1395–1406, Mar. 2016.
[158] J. C. Neely *et al.*, "Damping of inter-area oscillations using energy storage," in *Proc. IEEE Power Energy Soc. Gen. Meet. (PESGM)*. Vancouver, BC, Canada, Jul. 2013, pp. 1–5.
[159] North American Electric Reliability Corporation, "1996 System disturbances: Review of selected 1996 electric system disturbances in North America," North Amer. Elect. Rel. Corp., Princeton, NJ, USA, Tech. Rep., Aug. 2002.
[160] R. Elliott, R. Byrne, A. Ellis, and L. Grant, "Impact of increased photovoltaic generation on inter-area oscillations in the Western North American power system," in *Proc. IEEE Power Energy Soc. Gen. Meet. (PESGM)*, Washington, DC, USA, Jul. 2014, pp. 1–5.
[161] D. Trudnowski and J. Pierre, "Signal processing methods for estimating small-signal dynamic properties from measured responses," in *Inter-Area Oscillations in Power Systems*, A. R. Messina, Ed. New York, NY, USA: Springer, 2009.
[162] D. J. Trudnowski, D. Kosterev, and J. Undrill, "PDCI damping control analysis for the western North American power system," in *Proc. IEEE Power Energy Soc. Gen. Meet. (PES)* , Vancouver, BC, Canada, Jul. 2013, pp. 1–5.
[163] R. H. Byrne, D. J. Trudnowski, J. C. Neely, R. T. Elliott, D. A. Schoenwald, and M. K. Donnelly, "Optimal locations for energy storage damping systems in the Western North American interconnect," in *Proc. IEEE Power Energy Soc. Gen. Meet. (PES)*, Washington, DC, USA, Jul. 2014, pp. 1–5.
[164] D. A. Copp, F. Wilches-Bernal, I. Gravagne, and D. A. Schoenwald, "Time-domain analysis of power system stability with damping control and asymmetric feedback delays," in *Proc. 49th North Amer. Power Symp. (NAPS)*, 2017, pp. 1–5.
[165] North American Electric Reliability Corporation. *Eastern Interconnection Frequency Initiative White Paper*. Accessed: Apr. 12, 2017. [Online]. Available: http://www.nerc.com/pa/rrm/bpsa/Alerts%20DL/2015%20Alerts/EI%20 Frequency%20Initiative%20Whitepaper.pdf
[166] *Essential Reliability Services and the Evolving Bulk-Power System-Primary Frequency Response*. document RM16-6-000, FERC, 2016. [Online]. Available: https://www.ferc.gov/whats-new/comm-meet/2016/021816/E-2.pdf
[167] A. Oudalov, D. Chartouni, and C. Ohler, "Optimizing a battery energy storage system for primary frequency control," *IEEE Trans. Power Syst.*, vol. 22, no. 3, pp. 1259–1266, Aug. 2007.
[168] R. J. Concepcion, W. Wilches-Bernal, and R. H. Byrne, "Effects of communication latency and availability on synthetic inertia," in *Proc. 8th Conf. Innov. Smart Grid Technol. (ISGT)*, Arlington, VA, USA, Apr. 2017, pp. 1–5.
[169] G. Delille, B. Francois, and G. Malarange, "Dynamic frequency control support by energy storage to reduce the impact of wind and solar generation on isolated power system's inertia," *IEEE Trans. Sustain. Energy*, vol. 3, no. 4, pp. 931–939, Oct. 2012.
[170] N. W. Miller and K. Clark, "Advanced controls enable wind plants to provide ancillary services," in *Proc. IEEE Power Energy Soc. Gen. Meet. (PES)*, Minneapolis, MN, USA, Jul. 2010, pp. 1–6.
[171] L. Ruttledge and D. Flynn, "Emulated inertial response from wind turbines: Gain scheduling and resource coordination," *IEEE Trans. Power Syst.*, vol. 31, no. 5, pp. 3747–3755, Sep. 2016.
[172] Puerto Rico Electric Power Authority (PREPA). (2012). *Puerto Rico Electric Power Authority Minimum Technical Requirements for Photovoltaic Generation (PV) Projects*. [Online]. Available: http://www.fpsadvisorygroup.com/rso_request_for_quals/PREPA_Appendix_E_PV_Minimum_Technical_Requirements.pdf
[173] M. Lave, J. Kleissl, A. Ellis, and F. Mejia, "Simulated PV power plant variability: Impact of utility-imposed ramp limitations in Puerto Rico," in *Proc. IEEE 39th Photovolt. Specialists Conf. (PVSC)*, Tampa, FL, USA, Jun. 2013, pp. 1817–1821.
[174] Sentech, Inc., "Lessons learned: Planning and operating power systems with large amounts of renewable energy-based power generation," Hawaii Natural Energy Inst., Univ. Hawaii, Honolulu, HI, USA, Tech. Rep., Aug. 2012.
[175] J. Marcos, O. Storkël, L. Marroya, M. Garcia, and E. Lorenzo, "Storage requirements for PV power ramp-rate control," *Solar Energy*, vol. 99, pp. 28–35, Jan. 2014.
[176] A. Ellis, D. Schoenwald, J. Hawkins, S. Willard, and B. Arellano, "PV output smoothing with energy storage," in *Proc. 38th IEEE Photovolt. Specialists Conf.*, Austin, TX, USA, Jun. 2012, pp. 1523–1528.
[177] H. Ibrahim, A. Ilinca, and J. Perron, "Energy storage systems—Characteristics and comparisons," *Renew. Sustain. Energy Rev.*, vol. 12, no. 5, pp. 1221–1250, 2008.
[178] P. Mokrian and M. Stephen, "A stochastic programming framework for the valuation of electricity storage," in *Proc. 26th USAEE/IAEE North Amer. Conf.*, 2006, pp. 24–27.
[179] W. B. Powell and S. Meisel, "Tutorial on stochastic optimization in energy—Part I: Modeling and policies," *IEEE Trans. Power Syst.*, vol. 31, no. 2, pp. 1459–1467, Mar. 2016.
[180] M. Carrión and J. M. Arroyo, "A computationally efficient mixed-integer linear formulation for the thermal unit commitment problem," *IEEE Trans. Power Syst.*, vol. 21, no. 3, pp. 1371–1378, Aug. 2006.
[181] J. A. Muckstadt and R. C. Wilson, "An application of mixed-integer programming duality to scheduling thermal generating systems," *IEEE Trans. Power App. Syst.*, vols. PAS-87, no. 12, pp. 1968–1978, Dec. 1968, doi: 10.1109/TPAS.1968.292156.
[182] R. Jiang, J. Wang, and Y. Guan, "Robust unit commitment with wind power and pumped storage hydro," *IEEE Trans. Power Syst.*, vol. 27, no. 2, pp. 800–810, May 2012.
[183] J. Garcia-Gonzalez, R. M. R. D. L. Muela, L. M. Santos, and A. M. Gonzalez, "Stochastic joint optimization of wind generation and pumped-storage units in an electricity market," *IEEE Trans. Power Syst.*, vol. 23, no. 2, pp. 460–468, May 2008.
[184] Q. Wang, Y. Guan, and J. Wang, "A chance-constrained two-stage stochastic program for unit commitment with uncertain wind power output," *IEEE Trans. Power Syst.*, vol. 27, no. 1, pp. 206–215, Feb. 2012.
[185] D. Pozo, J. Contreras, and E. E. Sauma, "Unit commitment with ideal and generic energy storage units," *IEEE Trans. Power Syst.*, vol. 29, no. 6, pp. 2974–2984, Nov. 2014.
[186] R. Bellman, *Dynamic Programming*. Princeton, NJ, USA: Princeton Univ. Press, 1957.
[187] B. Cheng and W. Powell, "Co-optimizing battery storage for the frequency regulation and energy arbitrage using multi-scale dynamic programming," *IEEE Trans. Smart Grid*, to be published.
[188] B. D. Anderson and J. B. Moore, *Optimal Control, Linear Quadratic Methods*. Englewood Cliffs, NJ, USA: Prentice-Hall, 1990.
[189] S. Suhag and A. Swarup, "Intelligent load frequency control of two-area multi unit power system with SMES," in *Proc. 21st Int. Conf. Syst. Eng.*, Aug. 2011, pp. 147–152.

[190] M. Ahrens, L. Kucera, and R. Larsonneur, "Performance of a magnetically suspended flywheel energy storage device," *IEEE Trans. Control Syst. Technol.*, vol. 4, no. 5, pp. 494–502, Sep. 1996.
[191] J. Neely, J. Johnson, R. Byrne, and R. Elliott, "Structured optimization for parameter selection of frequency-watt grid support functions for wide-area damping," *Int. J. Distrib. Energy Resour. Smart Grids*, vol. 11, no. 1, pp. 69–94, 2015.
[192] J. D. Wolfe and D. F. Chichka, "An efficient design algorithm for optimal fixed structure control," in *Proc. 36th IEEE Conf. Decision Control*, vol. 3. Dec. 1997, pp. 2625–2627.
[193] J. M. Kanieski, H. A. Gründlinge, and R. Cardoso, "A new LQR modeling approach for power quality conditioning devices," in *Proc. 36th Annu. Conf. IEEE Ind. Electron. Soc. (IECON)*, Glendale, AZ, USA, Nov. 2010, pp. 2001–2006.
[194] W. B. Powell and S. Meisel, "Tutorial on stochastic optimization in energy—Part II: An energy storage illustration," *IEEE Trans. Power Syst.*, vol. 31, no. 2, pp. 1468–1475, Mar. 2016.
[195] J. B. Rawlings and D. Q. Mayne, *Model Predictive Control: Theory and Design*. San Francisco, CA, USA: Nob Hill, 2009.
[196] D. Q. Mayne, "Model predictive control: Recent developments and future promise," *Automatica*, vol. 50, no. 12, pp. 2967–2986, 2014.
[197] D. A. Copp and J. P. Hespanha, "Simultaneous nonlinear model predictive control and state estimation," *Automatica*, vol. 77, pp. 143–154, Mar. 2017.
[198] D. A. Copp and J. P. Hespanha, "Nonlinear output-feedback model predictive control with moving horizon estimation," in *Proc. IEEE 53rd Annu. Conf. Decision Control (CDC)*, Dec. 2014, pp. 3511–3517.
[199] M. Arnold and G. Andersson, "Model predictive control of energy storage including uncertain forecasts," in *Proc. Power Syst. Comput. Conf. (PSCC)*, Stockholm, Sweden, vol. 23. 2011, pp. 24–29.
[200] A. Parisio, E. Rikos, and L. Glielmo, "A model predictive control approach to microgrid operation optimization," *IEEE Trans. Control Syst. Technol.*, vol. 22, no. 5, pp. 1813–1827, Sep. 2014.
[201] I. Prodan and E. Zio, "A model predictive control framework for reliable microgrid energy management," *Int. J. Elect. Power Energy Syst.*, vol. 61, pp. 399–409, Oct. 2014.
[202] T. Wang, H. Kamath, and S. Willard, "Control and optimization of grid-tied photovoltaic storage systems using model predictive control," *IEEE Trans. Smart Grid*, vol. 5, no. 2, pp. 1010–1017, Mar. 2014.
[203] E. Perez, H. Beltran, N. Aparicio, and P. Rodriguez, "Predictive power control for PV plants with energy storage," *IEEE Trans. Sustain. Energy*, vol. 4, no. 2, pp. 482–490, Apr. 2013.
[204] A. D. Giorgio, F. Liberati, A. Lanna, A. Pietrabissa, and F. D. Priscoli, "Model predictive control of energy storage systems for power tracking and shaving in distribution grids," *IEEE Trans. Sustain. Energy*, vol. 8, no. 2, pp. 496–504, Apr. 2017.
[205] F. Sossan, E. Namor, R. Cherkaoui, and M. Paolone, "Achieving the dispatchability of distribution feeders through prosumers data driven forecasting and model predictive control of electrochemical storage," *IEEE Trans. Sustain. Energy*, vol. 7, no. 4, pp. 1762–1777, Oct. 2016.
[206] Indianapolis Power & Light Company. (2017). *Energy Storage*. [Online]. Available: https://www.iplpower.com/Our_Company/Environment/Energy_Storage/
[207] *Introduction to Wholesale Electricity Markets (WEM 101): Day-Ahead Energy Markets*, ISO-NE, Holyoke, MA, USA, Apr. 2017. [Online]. Available: https://www.iso-ne.com
[208] G. Strbac, "Demand side management: Benefits and challenges," *Energy Policy*, vol. 36, no. 12, pp. 4419–4426, Dec. 2008.
[209] P. Siano, "Demand response and smart grids—A survey," *Renew. Sustain. Energy Rev.*, vol. 30, pp. 461–478, Feb. 2014.
[210] J. S. Vardakas, N. Zorba, and C. V. Verikoukis, "A survey on demand response programs in smart grids: Pricing methods and optimization algorithms," *IEEE Commun. Surveys Tuts.*, vol. 17, no. 1, pp. 152–178, 1st Quart., 2015.
[211] P. Palensky and D. Dietrich, "Demand side management: Demand response, intelligent energy systems, and smart loads," *IEEE Trans. Ind. Informat.*, vol. 7, no. 3, pp. 381–388, Aug. 2011.
[212] H. Farhangi, "The path of the smart grid," *IEEE Power Energy Mag.*, vol. 8, no. 1, pp. 18–28, Jan./Feb. 2010.
[213] B. P. Roberts and C. Sandberg, "The role of energy storage in development of smart grids," *Proc. IEEE*, vol. 99, no. 6, pp. 1139–1144, Jun. 2011.
[214] A. Schroeder, "Modeling storage and demand management in power distribution grids," *Appl. Energy*, vol. 88, no. 12, pp. 4700–4712, 2011.
[215] A. Safdarian, M. Fotuhi-Firuzabad, and M. Lehtonen, "A distributed algorithm for managing residential demand response in smart grids," *IEEE Trans Ind. Informat.*, vol. 10, no. 4, pp. 2385–2393, Nov. 2014.
[216] L. Huang, J. Walrand, and K. Ramchandran, "Optimal demand response with energy storage management," in *Proc. IEEE 3rd Int. Conf. Smart Grid Commun. (SmartGridComm)*, Tainan, Taiwan, Nov. 2012, pp. 61–66.
[217] C. R. Touretzky and M. Baldea, "Integrating scheduling and control for economic MPC of buildings with energy storage," *J. Process Control*, vol. 24, no. 8, pp. 1292–1300, 2014.
[218] R. Halvgaard, L. Vandenberghe, N. K. Poulsen, H. Madsen, and J. B. Jørgensen, "Distributed model predictive control for smart energy systems," *IEEE Trans. Smart Grid*, vol. 7, no. 3, pp. 1675–1682, May 2016.
[219] M. Fiorentini, J. Wall, Z. Ma, J. H. Braslavsky, and P. Cooper, "Hybrid model predictive control of a residential HVAC system with on-site thermal energy generation and storage," *Appl. Energy*, vol. 187, pp. 465–479, Feb. 2017.
[220] X. Zhang, G. Hug, J. Z. Kolter, and I. Harjunkoski, "Model predictive control of industrial loads and energy storage for demand response," in *Proc. IEEE Power Energy Soc. Gen. Meet. (PESGM)*, Jul. 2016, pp. 1–5.
[221] K. Worthmann, C. M. Kellett, P. Braun, L. Grüne, and S. R. Weller, "Distributed and decentralized control of residential energy systems incorporating battery storage," *IEEE Trans. Smart Grid*, vol. 6, no. 4, pp. 1914–1923, Jul. 2015.
[222] E. R. Stephens, D. B. Smith, and A. Mahanti, "Game theoretic model predictive control for distributed energy demand-side management," *IEEE Trans. Smart Grid*, vol. 6, no. 3, pp. 1394–1402, May 2015.
[223] H. M. Soliman and A. Leon-Garcia, "Game-theoretic demand-side management with storage devices for the future smart grid," *IEEE Trans. Smart Grid*, vol. 5, no. 3, pp. 1475–1485, May 2014.
[224] W. Saad, Z. Han, H. V. Poor, and T. Basar, "Game-theoretic methods for the smart grid: An overview of microgrid systems, demand-side management, and smart grid communications," *IEEE Signal Process. Mag.*, vol. 29, no. 5, pp. 86–105, Sep. 2012.
[225] A.-H. Mohsenian-Rad, V. W. S. Wong, J. Jatskevich, R. Schober, and A. Leon-Garcia, "Autonomous demand-side management based on game-theoretic energy consumption scheduling for the future smart grid," *IEEE Trans. Smart Grid*, vol. 1, no. 3, pp. 320–331, Dec. 2010.
[226] I. Atzeni, L. G. Ordóñez, G. Scutari, D. P. Palomar, and J. R. Fonollosa, "Demand-side management via distributed energy generation and storage optimization," *IEEE Trans. Smart Grid*, vol. 4, no. 2, pp. 866–876, Jun. 2013.
[227] P. Vytelingum, T. D. Voice, S. D. Ramchurn, A. Rogers, and N. R. Jennings, "Agent-based micro-storage management for the smart grid," in *Proc. Int. Conf. Auto. Agents Multiagent Syst. (AAMAS)*, Toronto, ON, Canada, 2010, pp. 39–46.

RAYMOND H. BYRNE (F'17) received the B.S. degree in electrical engineering from the University of Virginia, the M.S. degree in electrical engineering from the University of Colorado, the M.S. degree in financial mathematics (financial engineering) from The University of Chicago, and the Ph.D. degree in electrical engineering from The University of New Mexico. He is currently a Distinguished Member of the Technical Staff at Sandia National Laboratories, where he has been employed since 1989. He currently serves as the Team Lead of the Equitable Regulatory Environment thrust area of the Sandia energy storage program. Awards include Time Magazine invention of the year in robotics in 2001 and the Prize Paper Award at the 2016 IEEE Power and Energy Society General Meeting for a paper on maximizing revenue from energy storage in grid applications. He is a member of Tau Beta Pi, Eta Kappa Nu, and Sigma Xi. He was elevated to IEEE Fellow for contributions to miniature robotics and grid integration of energy storage in 2017.

TU A. NGUYEN received the B.S degree in power systems from the Hanoi University of Science and Technology, Vietnam, in 2007, the Ph.D. degree from the Missouri University of Science and Technology, in 2014. He is currently a Post-Doctoral Appointee with the Energy Storage Technology and Systems Department, Sandia National Laboratories. From 2008 to 2009, he was a Power Transformer Test Engineer with the ABB High Voltage Test Department, Vietnam. From 2015 to 2016, he was a Post-Doctoral Research Associate with the University of Washington. His research interests include energy storage economics, microgrid modeling and analysis, and the integration of distributed resources into power grids.

DAVID A. COPP received the B.S. degree in mechanical engineering from The University of Arizona, Tucson, Arizona, in 2011, the M.S. and the Ph.D. degrees in mechanical engineering from the University of California at Santa Barbara, in 2014 and 2016, respectively. He was a member with the Center for Control, Dynamical-Systems, and Computation, University of California at Santa Barbara. He is currently a Post-doctoral Appointee with Sandia National Laboratories, where he works on grid integration, analysis, and control of energy storage. His broad research interests include control, modeling, analysis, and simulation of nonlinear and hybrid systems with applications to power and energy systems, multi-agent systems, robotics, and biomedicine.

BABU R. CHALAMALA (F'14) received the B.Tech. degree in electronics and communications engineering from Sri Venkateswara University, and the Ph.D. degree in physics from the University of North Texas. He is currently the Manager with the Energy Storage Technology and Systems Department, Sandia National Laboratories. He was a Corporate Fellow with SunEdison for five years, where he led Research and Development and product development in grid-scale energy storage. He founded two startup companies commercializing large format lithium batteries and digital x-ray sources. He was a Research Staff Member with Motorola, Research Triangle Institute, and Texas Instruments, where he made contribution to the development of electronic materials and device technologies. He is a Fellow Academy of Sciences St. Louis, a Life Member of the Electrochemical Society, and a Member of the Materials Research Society. As Chair of the IEEE Photonics Society Technical Committee on Displays, he was instrumental in launching the IEEE/OSA *J*ournal of Display Technology. He has been an active member of the Materials Research Society for twenty years and served as General Chair of the 2006 MRS Fall Meeting. He was a Guest Editor of the MRS Bulletin, Proceedings of the IEEE, and the IEEE JOURNAL ON SELECTED TOPICS in QUANTUM ELECTRONICS, and served on the editorial boards of the Proceedings of the IEEE and the IEEE ACCESS. He received the 2015 James Eads Award of the Academy of Sciences St. Louis.

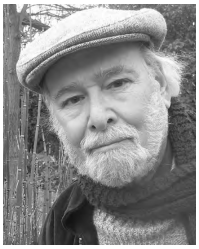

IMRE GYUK received the B.S. degree from Fordham University and the Ph.D. degree in theoretical physics from Purdue University. He was a Research Assistant with Brown University. He became a Research Associate with Syracuse University. He has taught physics, civil engineering, and architecture at the University of Wisconsin and Kuwait University. He currently directs the Energy Storage Research Program at the U.S. Department of Energy, funding work on a wide variety of technologies, such as advanced batteries, flywheels, and compressed air energy storage. Applications include improving grid resilience, making renewables dispatchable, helping to increase capacity factors, and easing congested distribution lines. His work has led to ten R&D 100 awards, the NAATBatt Lifetime Achievement Award, and the Phil Symons Energy Storage Award from the Energy Storage Association (ESA). He is internationally recognized as a leader in the energy storage field.